

RESEARCH

Open Access



The characteristic analysis of *TaTDF1* reveals its function related to male sterility in wheat (*Triticum aestivum* L.)

Sicong Shan^{1,3†}, Peng Tang^{1,3†}, Rui Wang^{1,3}, Yihang Ren^{1,3}, Baolin Wu^{1,3}, Nuo Yan^{1,3}, Gaisheng Zhang^{1,3}, Na Niu^{1,3*} and Yulong Song^{1,2,3*}

Abstract

Background The male sterile lines are an important foundation for heterosis utilization in wheat (*Triticum aestivum* L.). Thereinto, pollen development is one of the indispensable processes of wheat reproductive development, and its fertility plays an important role in wheat heterosis utilization, and are usually influencing by genes. However, these key genes and their regulatory networks during pollen abortion are poorly understood in wheat.

Results DEFECTIVE IN TAPETAL DEVELOPMENT AND FUNCTION 1 (TDF1) is a member of the R2R3-MYB family and has been shown to be essential for early tapetal layer development and pollen grain fertility in rice (*Oryza sativa* L.) and *Arabidopsis thaliana*. In order to clarify the function of TDF1 in wheat anthers development, we used *OsTDF1* gene as a reference sequence and homologous cloned wheat *TaTDF1* gene. TaTDF1 is localized in the nucleus. The average bolting time of *Arabidopsis thaliana* overexpressed strain (*TaTDF1*-OE) was 33 d, and its anther could be colored normally by Alexander staining solution, showing red. The dominant Mosaic suppression silence-line (*TaTDF1*-EAR) was blue-green in color, and the anthers were shrimpy and thin. The TaTDF1 interacting protein (TaMAP65) was confirmed using Yeast Two-Hybrid Assay (Y2H) and Bimolecular-Fluorescence Complementation (BiFC) experiments. The results showed that downregulated expression of *TaTDF1* and *TaMAP65* could cause anthers to be smaller and shrunken, leading to pollen abortion in *TaTDF1* wheat plants induced by virus-induced gene-silencing technology. The expression pattern of *TaTDF1* was influenced by *TaMAP65*.

Conclusions Thus, systematically revealing the regulatory mechanism of wheat *TaTDF1* during anther and pollen grain development may provide new information on the molecular mechanism of pollen abortion in wheat.

Keywords Wheat, Male sterility, Tapetum, Transcription factor, *TaTDF1*

[†]Sicong Shan and Peng Tang contributed equally to this work and should be considered co-first authors.

*Correspondence:

Na Niu
niuana@nwsuaf.edu.cn
Yulong Song
Sylbl1986@163.com

¹College of Agronomy, Northwest A&F University, Yangling, Shaanxi 712100, P.R. China

²State Key Laboratory of Crop Stress Biology for Arid Areas, Yangling, Shaanxi 712100, P.R. China

³National Yangling Agricultural Biotechnology & Breeding Center/ Yangling Branch of State Wheat Improvement Center/Wheat Breeding Engineering Research Center, Ministry of Education/Key Laboratory of Crop Heterosis of Shaanxi Province, Yangling, Shaanxi 712100, P.R. China



Background

Wheat is an important global food crop, and its yield plays an important role in stabilizing social and economic development and ensuring human health [1]. Therefore, it is important to use molecular biological technology to create excellent male-sterile lines and realize heterosis use to significantly increase the yield of wheat [2]. Male sterility is a complex physiological process involving the specific expression and silencing of many genes that can occur during differentiation of stamen into mature pollen grains [3]. It manifests as stamen degeneration or morphological abnormalities, meiosis abnormalities, microspore degeneration, tapetum cell function defects, and formation of fertile pollen without anther cracking [4]. In recent years, progress has been made in the study of key genes related to anther development and pollen formation in higher plants and their regulatory mechanisms in their networks. Several key genes involved in stamen development, pollen sac cell differentiation, pollen mother cell meiosis regulation, and the promotion of pollen wall formation and anther cracking have been identified in *Arabidopsis thaliana*, rice (*Oryza sativa* L.), and other plants [5].

R2R3-MYB belongs to one of the largest transcription factor (TF) families in the plant genome [6]. The N-terminus of R2R3-MYB comprises two homologous MYB domains (R2 and R3) that bind to specific target sequences through the synergistic effect of R2 and R3. Its C-terminus is a transcriptional regulatory region, and its sequence is rich in acidic amino acids that have transcriptional activation functions and participate in regulating the entire plant growth and development [7]. These include regulation of secondary metabolism, environmental factor response, development, and cell differentiation, and are especially for anther development and tapetum in higher plants [8, 9]. *AtMYB33* and *AtMYB65* are homologous to barley *GAMYB*. The tapetum cells of the *myb33* and *myb65* mutants increased abnormally during meiosis, leading to stagnation of microspore development in the prophase of meiosis [10]. *AtMYB21*, *AtMYB24*, and *AtMYB57* control the synthesis of lignin by interacting with hormones such as methyl jasmonate or by regulating the metabolic pathway of phenylpropane, thus regulating the dehiscence of anther [11–13]. *OsMYB103* positively regulates tapetum cell degradation by modulating the TFs ETERNAL TAPETUM 1 (EAT1) and PERSISTENT TAPETAL CELL 1 (PTC1), resulting in delayed tapetum cell degradation and pollen grain defects [14]. The mutant *pkSB* of *ZmMYB84* is characterized by thinning of the pollen outer wall, thickening and densification of the anther cuticle, and delayed degeneration of the tapetum cells. A study of its internal mechanism revealed that the *ZmMYB84-ZmPKSB* regulatory module could alter the expression of a series of genes

related to the biosynthesis and transportation of sporopollen, keratin, and wax. Furthermore, regulation of the formation of the anther cuticle and pollen outer wall helps maintain the normal development of pollen grains [15].

The *DYT1-TDF1-AMS-MS188-MS1* genetic pathway has been proved to regulate the development of *Arabidopsis thaliana* tapetum cells and play an important role in the normal degradation of anther tapetum cells. Abnormal expression of any transcription factor can cause pollen abortion [16]. *TDF1* belongs to the R2R3-MYB transcription factor family, which plays a role in the early development of tapetum layer. *AtTDF1* was found to be a key regulator in the early stages of the *Arabidopsis thaliana* anther tapetum, which can directly regulate *AtAMS*, thus regulating the development of tapetum cells and promoting pollen wall formation [17]. Cai et al. (2015) showed that overexpression of *OsTDF1* in *Arabidopsis thaliana tdf1* mutants can restore pollen fertility. The tapetum cells of *ostdf1* gene knockout mutant showed a vacuolation phenotype similar to *Arabidopsis thaliana tdf1* mutant, which caused male sterility [18]. *AtTDF1* is a negative regulator of ascorbic acid (vitamin C) accumulation in *Arabidopsis thaliana* anthers, which prevents tapetum cells from excessive division. It affects ROS homeostasis in anthers by mediating antioxidant L-ascorbic acid content, thus promoting tapetum cell division and differentiation [19]. Moriyama et al. (2022) successfully transformed the allele of the male sterility gene *lftdf1* into Easter lilies using a hybridization test and observed the pollen sterility phenotype [20]. However, there are few reports on genes related to pollen abortion during anther development in wheat. Wu et al. (2023) found that both *TaTDRL-EAR* and *TaMYB103-EAR* transgenic *Arabidopsis thaliana* plants showed abnormal pollen phenotypes, abortions, and low seed-setting rates. The homolog of the *TaTDRL* gene in *Arabidopsis thaliana* is *AtAMS*, which is the downstream TF of *TaTDF1* [21].

In this study, *OsTDF1* protein sequence of rice was used as reference, and homologous *TaTDF1* was identified in wheat by homologous alignment. The gene structure, protein structure, physical and chemical properties, phylogeny, expression level and subcellular localization of *TaTDF1* were studied. Furthermore, the interacting proteins were screened by the Y2H. Moreover, *TaTDF1* transgenic *Arabidopsis thaliana* plants and *TaTDF1* silences in wheat were generated to clarify the molecular mechanism of *TaTDF1* in the regulation of the wheat pollen abortion process. This study helps build a solid theoretical foundation for the subsequent creation of new excellent wheat male-sterile lines.

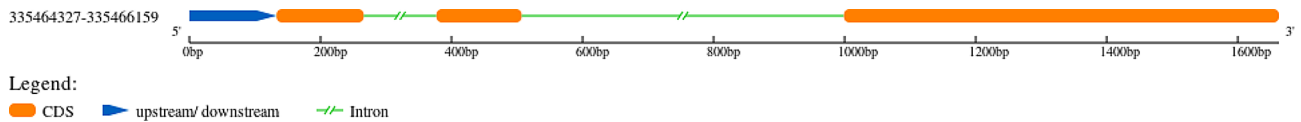


Fig. 1 *TaTDF1* gene structure analyses. Orange boxes indicate exons encoding amino acids and green lines indicate introns. Blue represents the untranslated region. Numbers represent the lengths of each region in base pairs

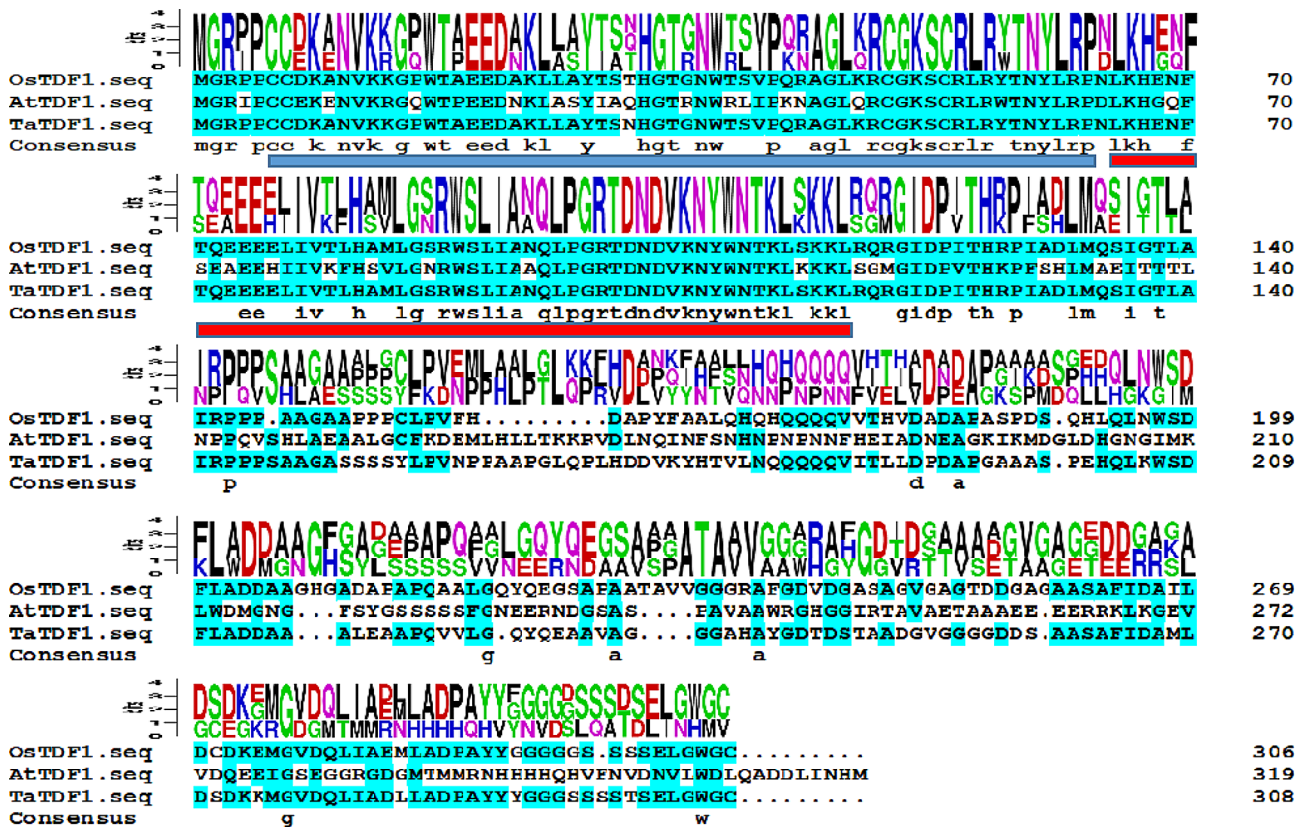


Fig. 2 Protein sequence analysis of TaTDF1. Multiple alignment of TaTDF1 other basic R2R3-MYB domain proteins comprising Arabidopsis thaliana defective in tapetal development and function 1 (AtTDF1) and Oryza sativa L. defective in tapetal development and function 1 (OsTDF1). The highly conserved amino acid residues among the proteins examined are shaded. The solid Blue line shows the R2 domain (6–63 aa).The solid Red line shows the R3 domain (65–116 aa)

Results

Cloning and sequence analysis of TaTDF1

The protein sequence of OsTDF1 was taken as reference, and same-source comparison was performed using Ensemble Plants database. The cause with the lowest E-val and highest Score (TraesCS4D02G192400.1) was used as the target sequence. The sequence was further checked and calibrated by Protein BLAST in NCBI database, and finally the *TaTDF1*-4D (hereinafter referred to as *TaTDF1*) gene was determined as the research object. In this study, the wheat K-type cytoplasmic male-sterile line MS (Kots) -90-110 (MS) and its fertile control line MR (Kots) -90-110 (MF) were used. Using MF-90-110 meiosis anthesis cDNA as a template, the target band was amplified to 924 bp, encoding 308 amino acid residues. The molecular weight of the protein was approximately

32.9 kDa, pI=5.46 (Table S3). *TaTDF1* contains three exons, two introns and the conserved domain spans amino acids 6-116 aa (Figs. 1 and 2). Cluster X multi-sequence alignment showed that the similarity of protein sequences between TaTDF1, OsTDF1, and AtTDF1 was 75.24% and 33.02%, respectively. Phylogenetic tree analysis of TaTDF1 using MEGA showed that TaTDF1 was closely related to barley (*Hordeum vulgare* L., XP.044979101.1). It is relatively conserved on homologous chromosomes A, B, and D (Fig. 3). The prediction of the secondary structure of TaTDF1 in the protein showed that the helix accounted for 38.31%, the random curl for 46.10%, extended chain accounted for 7.79%, and the turn for 7.79% (Fig. S1).

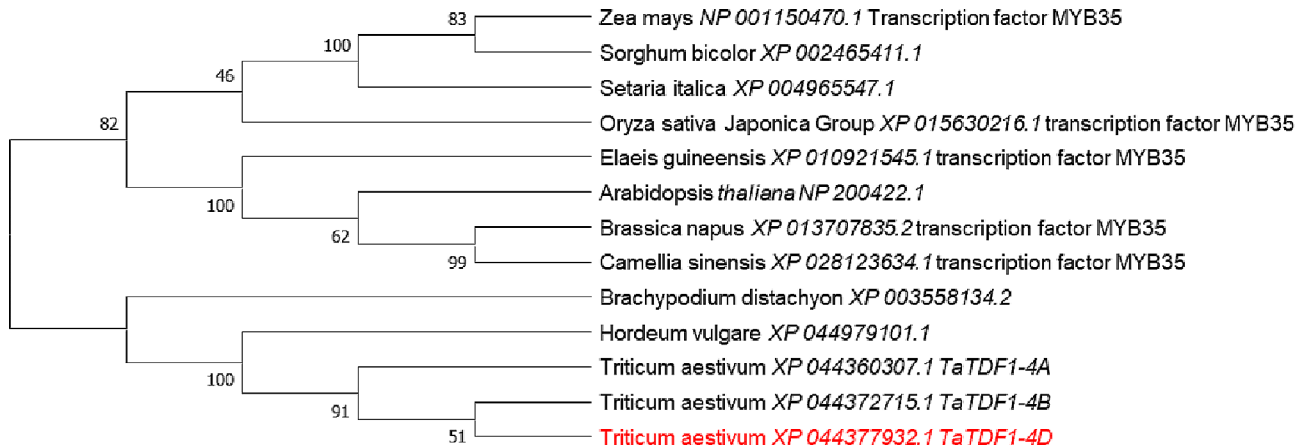


Fig. 3 Phylogenetic analysis of TaTDF1. Phylogenetic tree analysis of TaTDF1 using Neighbor-joining method by MEGA-X program. Bootstrap values from 1000 replicates were indicated at each node

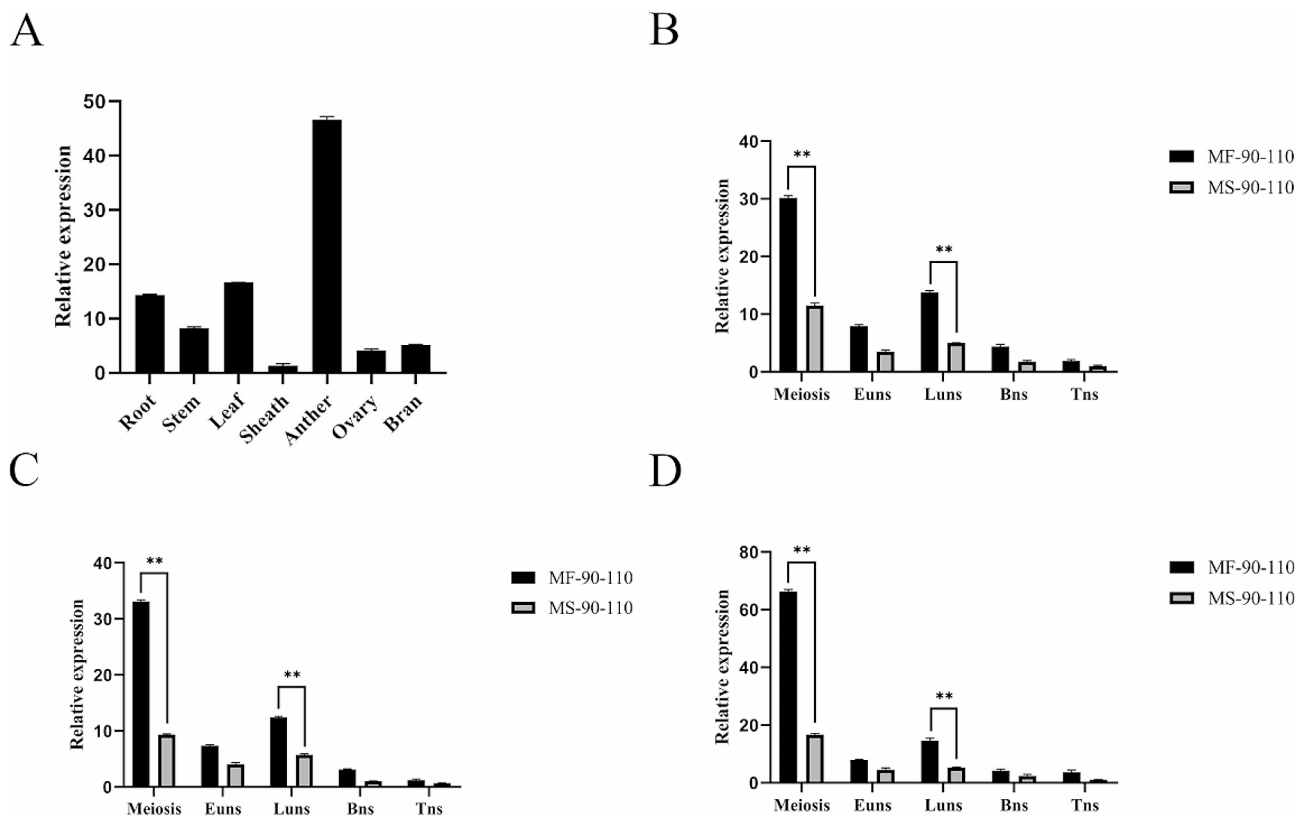


Fig. 4 The expression patterns of TaTDF1. (A) The expression pattern of TaTDF1 in various tissues in MS-90-110 and MF-90-110. (B) The expression levels of TaTDF1-4A in MS-90-110 and MF-90-110 during anther development. (C) The expression levels of TaTDF1-4B in MS-90-110 and MF-90-110 during anther development. (D) The expression levels of TaTDF1-4D in MS-90-110 and MF-90-110 during anther development. EUns: Early uninucleate stage; LUns: Late uninucleate stage; Bns: Binucleate stage; Tns: Trinucleate stage. Data was presented as the means \pm SD of three technical replicates and three biological replicates. The significance of differences was assessed using the Student's t-test. ** $p < 0.05$

The expression pattern analysis of TaTDF1

TaTDF1 expression levels in different tissues and anthers of MS-90-110 and MF-90-110 cells at different developmental stages were analyzed using real-time fluorescence quantitative polymerase chain reaction (qRT-PCR). The results showed that the expression level of TaTDF1 in

anthers was significantly higher than that in other tissues. Expression levels in the leaf sheath, ovary, and bran were relatively low (Fig. 4A). The expression of TaTDF1-4A, TaTDF1-4B and TaTDF1-4D decreased first, then increased, and finally decreased in the five stages of anther development. The expression levels of each gene

in MF-90-110 anthers were higher than those in MS-90-110 anthers. During meiosis, the expression levels of *TaTDF1-4A*, *TaTDF1-4B* and *TaTDF1-4D* in the anthers of MF-90-110 were significantly higher than those of MS-90-110, and the expression levels of *TaTDF1-4D* were significantly higher than those of *TaTDF1-4A* and *TaTDF1-4B*. (Figure 4B, C and D). These results suggest that the differential expression of *TaTDF1* in sterile and fertile lines during meiosis may be related to anther development and pollen grain fertility.

35 S: EGFP and 35 S: TaTDF1-EGFP were transformed into *Agrobacterium tumefaciens* and injected into tobacco epidermal cells. The transient expression results showed that 35 S: EGFP produced signals of green fluorescent proteins in the cytoplasm and nucleus. However, 35 S: TaTDF1-EGFP exhibited only green fluorescence in the nucleus (Fig. 5).

Yeast two hybridization (Y2H) screening of interacting proteins that bind to the TaTDF1 protein

To verify whether TaTDF1 has toxic and transcriptional activation functions, we tested its transcriptional activation activity by constructing the yeast expression vector BD-TaTDF1. PGBKT7 (BD) and BD-TaTDF1 were transformed into yeast-competent cells Y2H, respectively. The colonies of BD and BD-TaTDF1 were white and there was no obvious difference in growth (Fig. 6A). At the same time, BD-TaTDF1 of $OD_{600}=0.85$. These results showed that BD-TaTDF1 was not toxic to yeast cells. Negative

control BD and target protein BD-TaTDF1 can be grown only on the SD/-Trp medium, not SD/-Trp/-Ade/-His medium. The positive control P53 was grown on SD/-Trp and SD/-Trp/-Ade/-His media. These results indicate that BD-TaTDF1 does not have transcriptional activation activity and can be used for verification of yeast interactions and library screening (Fig. 6B).

The wheat anther cDNA library plasmids were transformed into yeast cells containing the bait vector BD-TaTDF1 and the products were coated onto SD/-Ade/-His/-Leu/-Trp and SD/-Ade/-His/-Leu/-Trp/X- α -gal media for screening. Therefore, 25 well-growing colonies with a bluish color were obtained (Fig. 6C). Twenty-five positive clones were amplified, plasmids were extracted, and sent to Shanghai Sangon Biotech for sequencing. The sequencing results were compared with those from the Ensembl Plants and NCBI databases. Seventeen non-redundant proteins were obtained, and their functions were further annotated (Table S3). These 17 proteins are involved in multiple metabolic pathways. TaMAP65, a protein screened for microtubule kinetic arrays associated with the microspore nuclear division process, was used as a candidate interaction protein.

Cloning and sequence analysis of TaMAP65

A candidate interacting protein of TaMAP65 was screened by the yeast two hybrid with an annotation of the MAP65_ASE1 superfamily (TraesC-S1A02G256800.1). The full-length CDS of the *TaMAP65*

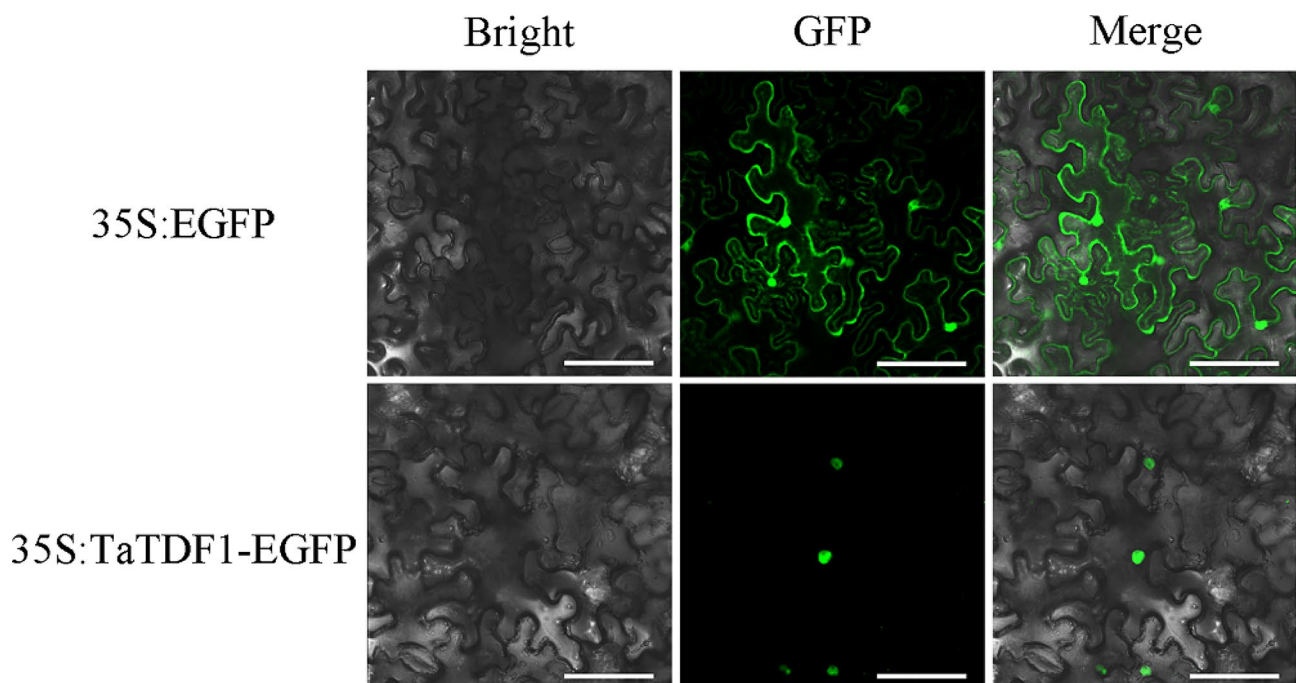


Fig. 5 The subcellular location of TaTDF1 protein as GFP fusions. Subcellular localization of TaTDF1-enhance green fluorescence protein (EGFP) fusion protein in tobacco epidermal cells. Scale bars = 50 μ m

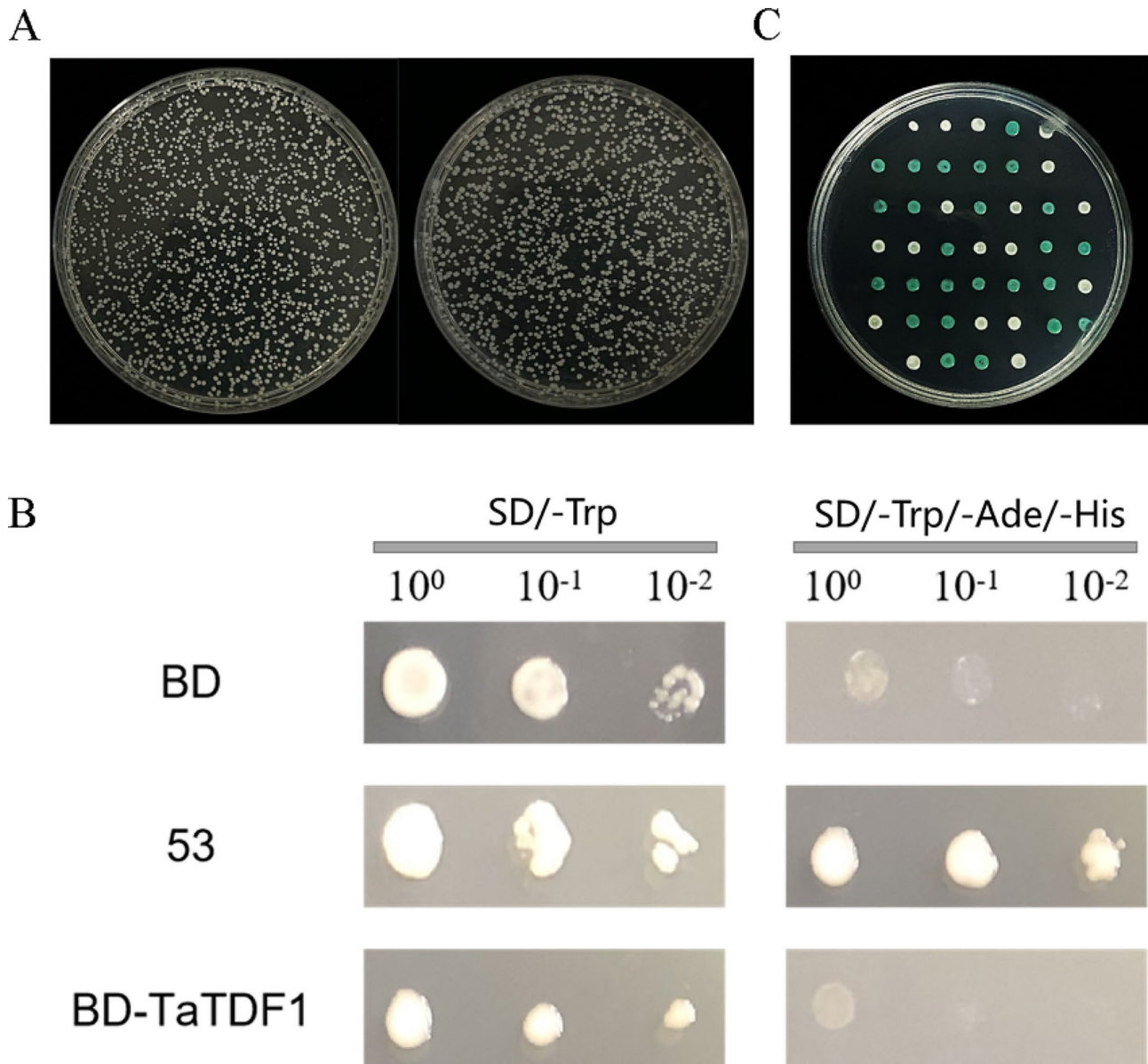


Fig. 6 (A) Trans-activation activity and Y2H assay in the yeast system. TaTDF1 protein yeast toxicity assay. BD empty vector and yeast cells containing BD-TaTDF1 bait vector are cultured on SD/-Trp plates. On the left is BD and on the right is BD-TaTDF1. (B) Trans-activation assay of the TaTDF1 proteins. Full-length of TaTDF1 were fused with the GAL4 DNA-binding domain, and then expressed in yeast strain Y2H. The transformed yeast cells were plated and grown on control plates (SD/-Trp) or selective plates (SD/-Trp-His-Ade + X- α -gal). (C) The screening of interacted proteins with TaTDF1. The wheat anthers cDNA library plasmid was transformed into yeast cells containing the decoy vector BD-TaTDF1, and the transformation product was coated onto SD/-Ade/-His/-Leu/-Trp + X- α -gal plates

gene is 2034 bp, encoding 677 aa. The molecular weight of the protein is approximately 76.15 kDa, and the pI=6.07 (Table S3). The 5' and 3' untranslated regions (UTR) of the *TaMAP65* gene are 161 bp and 306 bp, respectively (Fig. 7). Cluster X multisequence alignment showed that the sequence similarities of the TaMAP65, OsMAP65, and AtMAP65 proteins were 70.58% and 49.09% (Fig. 8), respectively. Using MEGA.X, we studied the evolutionary relationship of TaMAP65 and found that TaMAP65 is closely related to the evolutionary relationship of

Aegilops tauschii Coss (XP.040246772.1) and is relatively conserved on the homologous A, B and D chromosome (Fig. 9). The secondary structure of TaMAP65 in the protein showed that helix accounted for 59.38%, random curl accounted for 34.12%, extended chain accounted for 3.84% and turn accounted for 2.66% (Fig. S2).

Analysis of TaMAP65 expression pattern

The expression levels of *TaMAP65* in different tissues and anthers of MS-90-110 and MF-90-110 in different

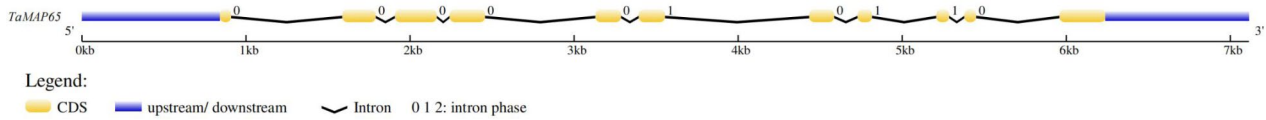


Fig. 7 Gene structure of *TaMAP65*. Yellow boxes indicate exons encoding amino acids and Black lines indicate introns. Blue represents the untranslated region. Numbers represent the lengths of each region in base pairs

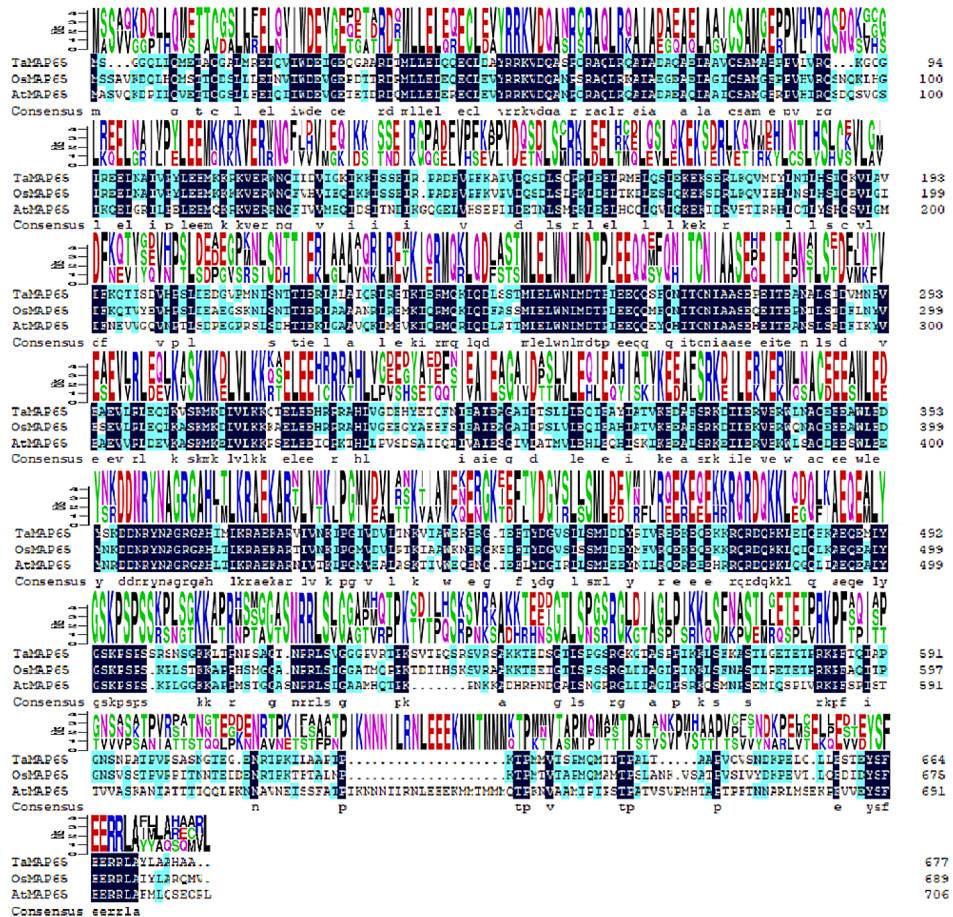


Fig. 8 Protein sequence analysis of *TaMAP65* protein. Multiple alignment of *TaMAP65* and other basic *MAP65_ASE1* domain proteins comprising *AtMAP65* and *OsMAP65*. The highly conserved amino acid residues among the proteins examined are shaded

developmental stages were analyzed using qRT-PCR. The expression level of *TaMAP65* in the anther was significantly higher than the other tissues. However, the expression levels in the ovary and bran were relatively low (Fig. 10A). *TaMAP65*-1 A, *TaMAP65*-1B, and *TaMAP65*-1D were detected in MS-90-110. Meanwhile, the expression levels of *TaMAP65*-1 A and *TaMAP65*-1B were decreased from meiosis to trinucleate stage. However, the *TaMAP65*-1D were decreased from meiosis to late uninucleate stage, and then increased sharply at binucleate stage. Whereafter, the expression levels of *TaMAP65*-1D was persisting declination. Furthermore, their expression levels in the anthers of MF-90-110 during meiosis and early uninucleate stage were significantly higher than

those in MS-90-110 except *TaMAP65*-1D (Fig. 10B, C and D). *TaMAP65* has been speculated to be involved in the development of anther and pollen fertility. 35 S: EGFP and 35 S: *TaMAP65*-EGFP were transformed into *Agrobacterium tumefaciens* and injected into tobacco epidermal cells. The results of transient expression showed that a signal of green fluorescent protein was observed in the cytoplasm and nucleus of 35 S: EGFP. However, 35 S: *TaMAP65*-EGFP exhibited only a green fluorescence signal in the nucleus (Fig. 11).

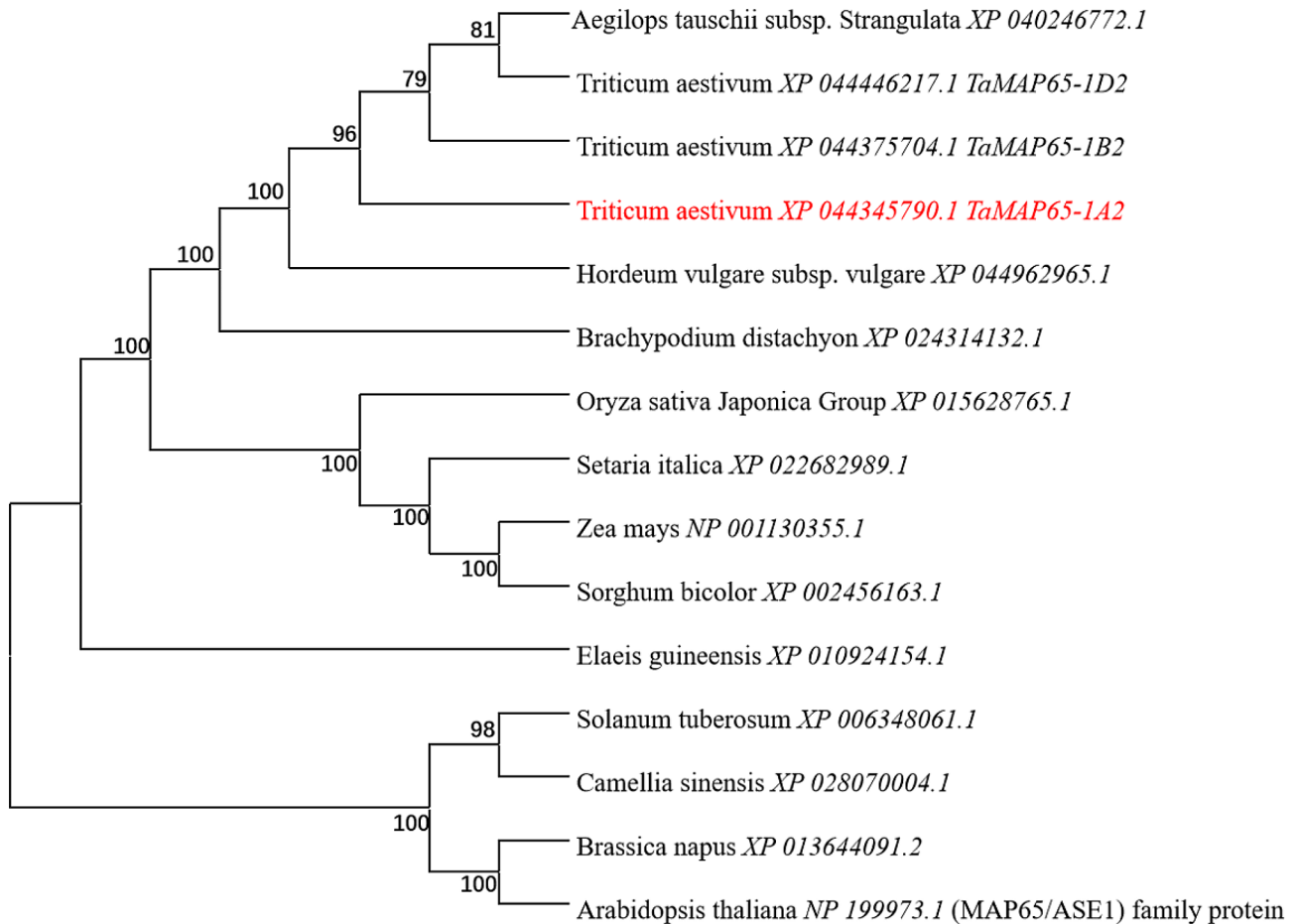


Fig. 9 Phylogenetic analysis of TaMAP65. Phylogenetic tree analysis of TaMAP65 using Neighbor-joining method using MEGA-X program. Bootstrap values from 1000 replicates were indicated at each node

Verification of the interaction between the TaTDF1 and TaMAP65 protein

To further confirm the interaction between TaMAP65 and TaTDF1, recombinant vectors AD-TaMAP65 and BD-TaTDF1 were co-transformed into yeast-competent Y2H cells. AD-T+BD-Lam and AD-T+BD-53 cells were used as negative and positive controls, respectively. The results showed that the combination of the positive controls AD-T+BD-53 and BD-TaTDF1+AD-TaMAP65 grew on SD/-Trp/-Ade/-Leu/-His medium, and the colonies were blue. The negative control, AD-T+BD-Lam, did not grow on the SD/-Trp/-Ade/-Leu/-His medium (Fig. 12A and B). These results show that there is an interaction between the TaTDF1 and TaMAP65 proteins.

pUN-SPYNE, pUC-SPYCE, pUN-TaTDF1, and pUC-TaMAP65 were transformed into the *Agrobacterium tumefaciens* strain GV3101 (pSoup-19) and transiently expressed in *Nicotiana tabacum* leaves. The interaction between TaTDF1 and TaMAP65 was observed under a laser confocal microscope, in which TaTDF1-SPYNE+pUC-SPYCE and pUN-SPYNE+TaMAP6-SPYCE were used as negative controls. The results

showed that there was no green fluorescent protein (GFP) fluorescence signal in negative control tobacco cells; however, there was a green fluorescence signal in the nucleus of the pUN-TaTDF1+pUC-TaMAP65 experimental group, indicating that TaTDF1 and TaMAP65 proteins could interact with the nucleus (Fig. 13).

Functional analysis of TaTDF1 in *Arabidopsis thaliana*

In order to further analyze the function of *TaTDF1* gene in anther or pollen development, this study studied heterologous high expression of *TaTDF1*-OE and dominant chimeric inhibitory silencing gene *TaTDF1*-EAR in *Arabidopsis thaliana*, and obtained *TaTDF1*-OE overexpression lines and *TaTDF1*-EAR dominant chimeric inhibitory silencing lines, respectively. By observing the phenotype, it was found that compared with wild *Arabidopsis thaliana*, *TaTDF1*-OE overexpression lines and *TaTDF1*-EAR dominant chimeric suppression silent lines also bloomed normally (Fig. 14A). The average bolting time was 33 d in *TaTDF1* overexpression (*TaTDF1*-OE) *Arabidopsis thaliana* plants, which was significantly earlier than in wild-type *Arabidopsis thaliana* plants by

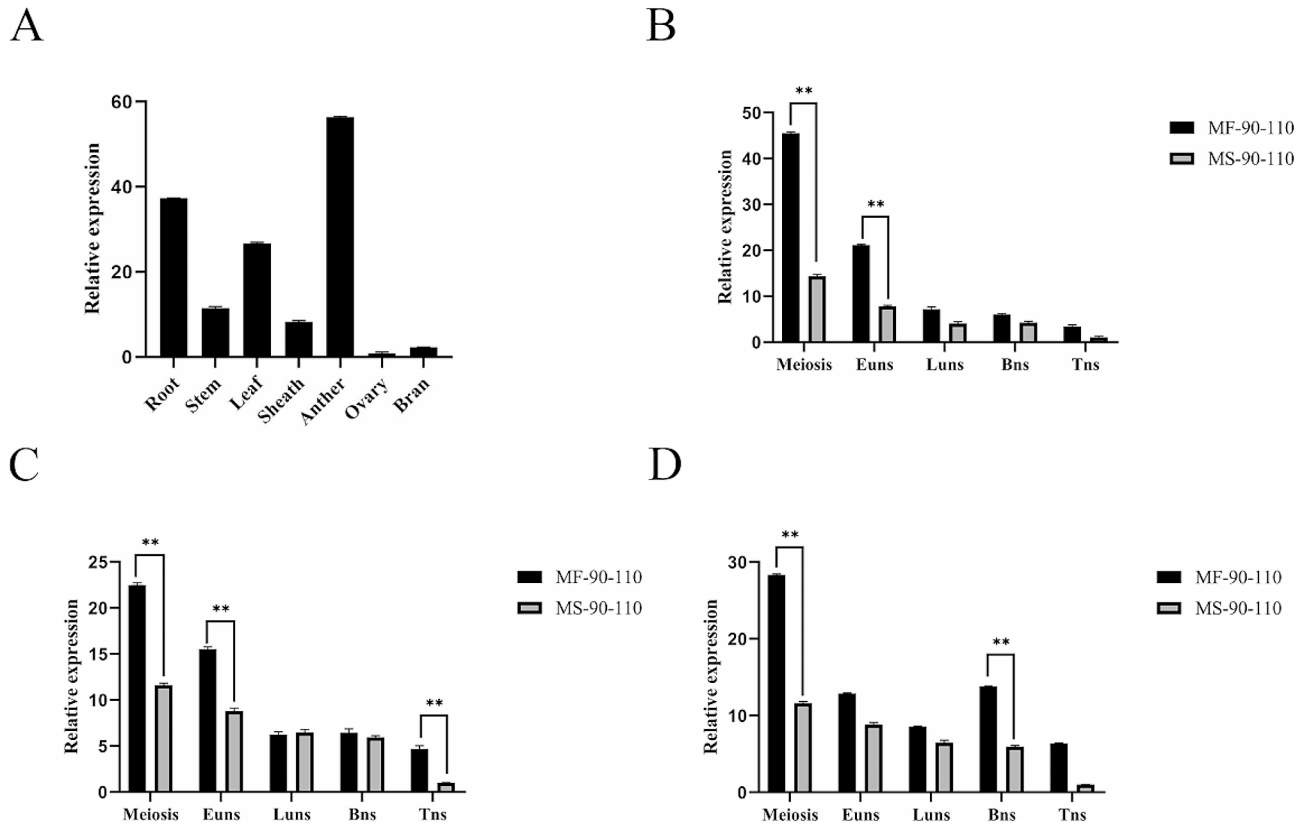


Fig. 10 The expression patterns of *TaMP65*. **(A)** The expression pattern of *TaMP65-1A* in various tissues in MS-90-110 and MF-90-110. **(B)** The expression levels of *TaMP65-1A* in MS-90-110 and MF-90-110 during anther development; **(C)** The expression levels of *TaMP65-1B* in MS-90-110 and MF-90-110 during anther development. **(D)** The expression levels of *TaMP65-1D* in MS-90-110 and MF-90-110 during anther development. EUn: Early uninucleate stage; LUn: Late uninucleate stage; Bns: Binucleate stage; Tns: Trinucleate stage. Data was presented as the means ± SD of three technical replicates and three independent biological replicates. The significance of differences was assessed using the Student's t-test. ** $p < 0.05$

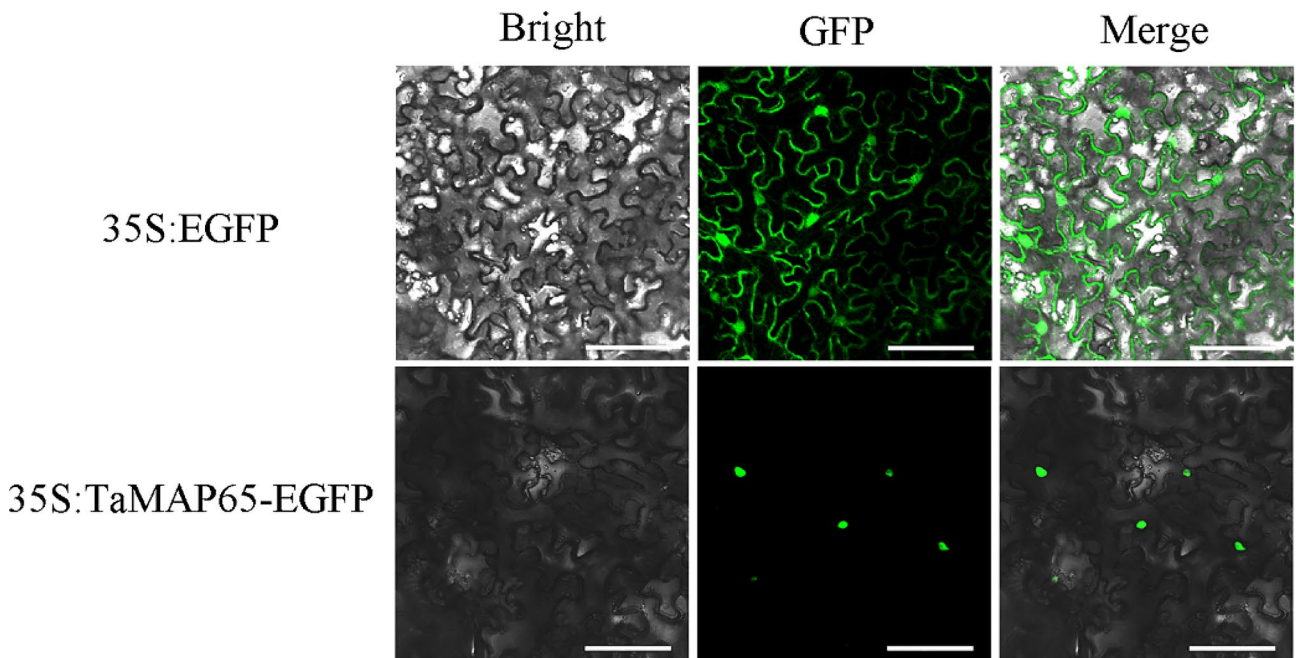


Fig. 11 The subcellular location of TaMAP65 protein. Subcellular localization of TaMAP65-enhance green fluorescence protein (EGFP) fusion protein in tobacco epidermal cells. Scale bars = 50 μ m

A



B

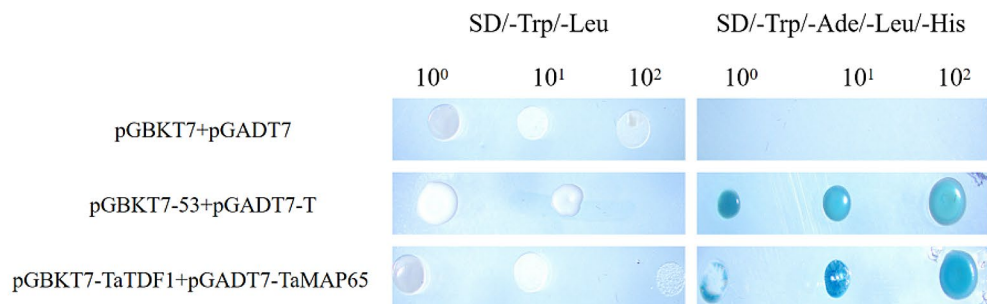


Fig. 12 The interaction between TaTDF1 with TaMAP65. **(A-B)** Yeast two-hybrid assay to test the interaction of TaTDF1 with TaMAP65. The BD-TaTDF1 recombinant plasmid and AD-TaMAP65 recombinant plasmid were co-transformed into Y2H yeast cells. The bacterial solution was located on SD/-Trp/-Leu/-Ade/-His solid medium

approximately 7 d (Fig. 14B and C). Wild *Arabidopsis thaliana* and *TaTDF1*-OE plant anther can be colored normally by Alexander staining solution and appear red (Fig. 14D and E). The average bolting period in dominant chimerism inhibition-silenced *Arabidopsis thaliana* plants (*TaTDF1*-EAR) was approximately 4 d later than that in wild-type *Arabidopsis thaliana* plants (Fig. 14B and C). The anthers from *TaTDF1*-EAR plants were shrunken and small and showed a blue-green color upon staining with Alexander's stain (Fig. 14F). The above results indicated that overexpression of allogenic transcription factor *TaTDF1* in *Arabidopsis thaliana* resulted in normal fertility of pollen grains, while silenced allogenic transcription factor *TaTDF1* resulted in withered, thin and sterile pollen grains, indicating that transcription factor *TaTDF1* is essential for pollen development in *Arabidopsis thaliana*. It is an important positive regulatory protein factor to maintain the normal development of pollen grains.

Functional analysis of TaTDF1 and TaMAP65 in wheat

In this study, γ -*PDS*, γ -*TaTDF1* and γ -*TaMAP65* recombinant plasmids were constructed, the MF-90-110 wheat leaves were inoculated with Barley Stripe Mosaic Virus (BSMV)-Based Virus-Induced Gene Silencing (VIGS) technology. The phenotype of the leaves was observed 10 d after inoculation, anther morphology and pollen fertility were observed in the flowering stage, and the expression levels of *TaTDF1* and *TaMAP65* were analyzed.

The leaves of wheat inoculated with barley stripe mosaic virus BSMV: *PDS* showed photobleaching, whereas those inoculated with BSMV:00, BSMV:*TaTDF1* or BSMV:*TaMAP65* showed striped lesions (Fig. 15A). Thus, the technical system for BSMV induced wheat *TaTDF1* and *TaMAP65* gene silencing was reliable. The silencing efficiency of *TaTDF1* in *tatdf1* silencing strain was 0.095 and that of *TaMAP65* was 0.96 (Fig. 15B). The silencing efficiency of *TaTDF1* in the *tamap65* silencing strain was 0.108 and that of *TaMAP65* was 0.151 (Fig. 15C). Compared with the BSMV:00 negative control plants, the expression levels of *TaTDF1* and the *TaMAP65* genes decreased significantly (Fig. 15B and C). Investigation of the panicle seed-setting rate in BSMV:*TaTDF1* and BSMV: *TaMAP65* silenced plants, which revealed that the seed-setting rate of BSMV:*TaTDF1* was the lowest (Fig. 15D). Downregulation of *TaTDF1* and *TaMAP65* significantly reduced grain fertility, suggesting that the expression of *TaTDF1* and *TaMAP65* could be closely related to pollen fertility.

In order to further study the regulatory effect of *TaTDF1* gene on wheat anther development, this study used cDNA of wheat WT plant and *tatdf1* mutant as templates, and analyzed the expression patterns of a series of downstream genes related to tapetum development of *TaTDF1* gene by qRT-PCR. The results showed that, in comparison with WT plants, the expression of *TaAMS*, *TaMYB80* and *TaMS1* genes in *tatdf1* mutant is down-regulated by about 85%, suggesting that anther

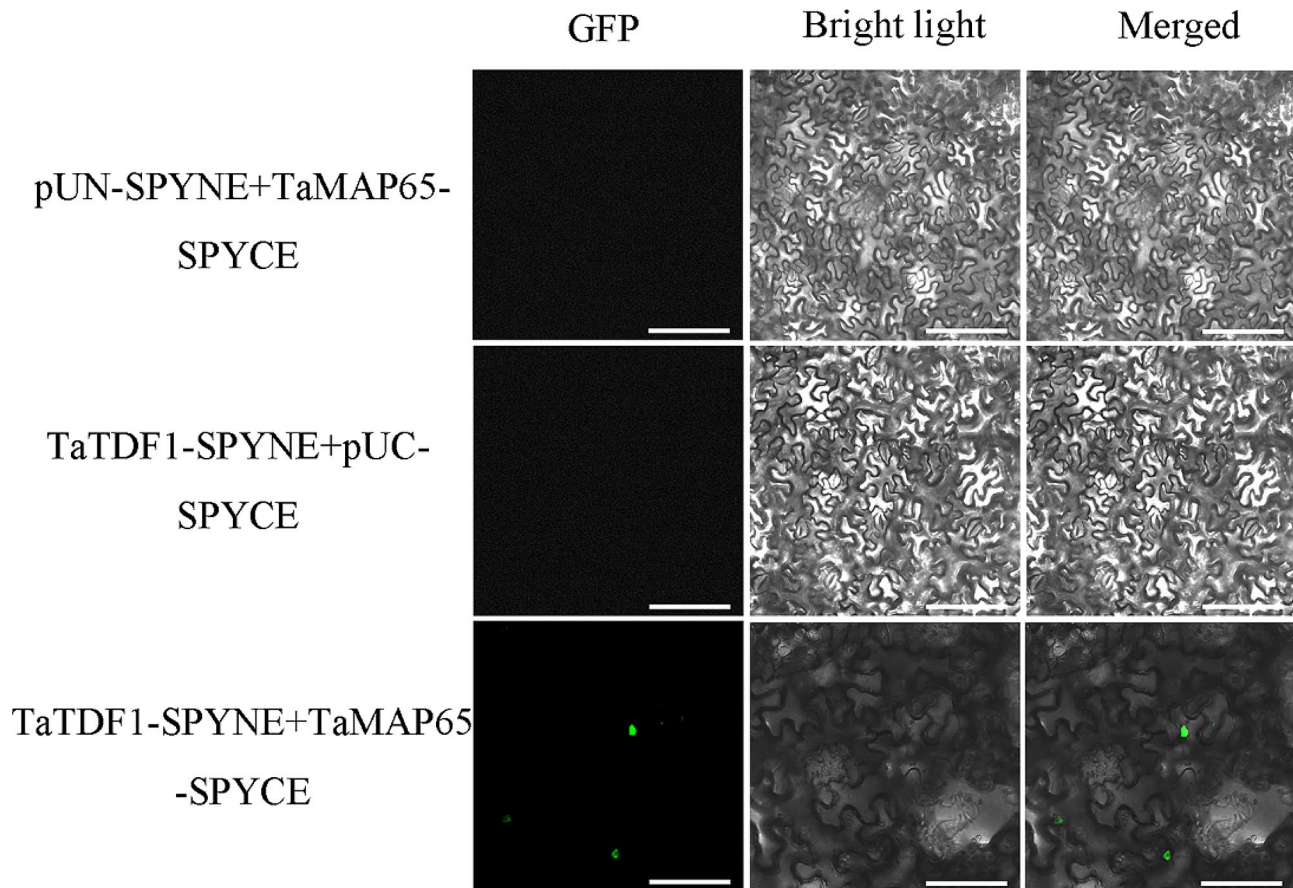


Fig. 13 The bi-molecular fluorescence complementation (BiFC) assay of TaTDF1 with TaMAP65. The full-length TaTDF1 and TaMAP65 were cloned into pUN-SPYNE and pUC-SPYCE, respectively. The recombinant constructs were transiently expressed in tobacco leaves by agroinfiltration. Scale bars = 50 μ m

abortion in *tatdf1* mutant may be accompanied by abnormal tapetum cell development (Fig. 16). This point needs to be further studied.

Karyotypes and fertility of the anthers and pollen grains of MOCK, BSMV:00, BSMV: *PDS*, BSMV: *TaTDF1*, and BSMV: *TaMAP65* plants in the pollen-scattering stage were observed (Fig. 17 A1-A5). Compared with MOCK, BSMV: *PDS*, and BSMV:00, the anthers of BSMV: *TaTDF1* and BSMV: *TaMAP65* were shriveled, thin, and dull during the pollen-scattering stage (Fig. 17 B1-B5, Fig. 17 C1-C5). Using 10 g/mL of DAPI dye solution to detect the karyotype of pollen grains in the loose pollen stage, the pollen grains of the MOCK, BSMV: *PDS*, and BSMV:00 plants developed into fish-like sperm nuclei (Fig. 18 A1-A3). However, the pollen grains of BSMV: *TaTDF1* and BSMV: *TaMAP65* were abnormal, and most were seedless, and few developed into fish-like sperm nuclei (Fig. 18 A4, 17 A5). The pollen grains of MOCK, BSMV:00, and BSMV: *PDS* plants were stained with 1% I₂-KI solution and blue-black (Fig. 18 B1-B3). However, most pollen grains of the BSMV: *TaTDF1* and BSMV: *TaMAP65* were stained with 1% I₂-KI solution, although some pollen grains were still stained blue-black

(Fig. 18 B4, Fig. 18B5). Therefore, *TaMAP65* could be located upstream of *TaTDF1*, and the downregulated expression of *TaTDF1* and *TaMAP65* could affect the development of the anther, causing starch in pollen grains to accumulate with difficulty, thus causing pollen grains to abort.

Discussion

Pollen grains are important to plant male reproductive organs. The growth and development of pollen grains are closely related to the differentiation of the microspore mother cells, the degradation of the tapetum cells, and the formation of the callose and pollen walls [22]. Mutations in genes related to pollen grain development or environmental changes can also cause abnormal pollen development, resulting in male sterility. Previous studies have found that the *DYT1-TDF1-AMS-MYB80* gene pathway strictly controls tapetum development and plays an important role in maintaining normal degradation of tapetum cells and ensuring pollen fertility. This has been confirmed in *Arabidopsis thaliana*, rice, tomatoes (*Solanum lycopersicum* L.), and asparagus (*Asparagus officinalis* L.) [23–26].

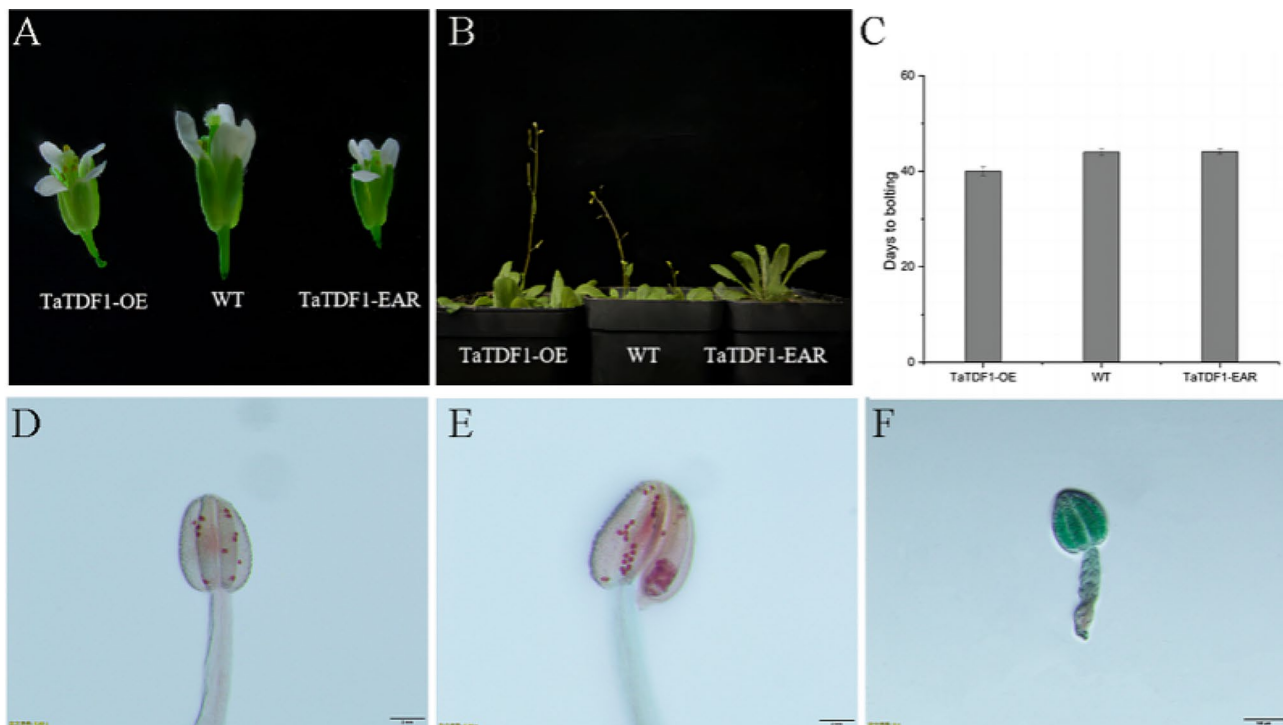


Fig. 14 Homotypic analyses of *TaTDF1*-OE, wild-type, *TaTDF1*-EAR plant. **(A)** Phenotype of flowers from *TaTDF1*-OE, wild-type, *TaTDF1*-EAR plant. **(B)** Phenotype of plant from *TaTDF1*-OE, wild-type, *TaTDF1*-EAR plant. **(C-E)** Alexander staining of anther from from *TaTDF1*-OE, wild-type, *TaTDF1*-EAR plant, respectively. **(F)** The days to bolting of plant from *TaTDF1*-OE, wild-type, *TaTDF1*-EAR plant; Scale bars = 50 μm in **(C-E)**.

The *TDF1* gene belongs to the *DYT1-TDF1-AMS-MYB80* pathway. Mutation or deletion of its base sequence leads to abnormal degradation of tapetum cells, leading to an imbalance in nutrient metabolism and, eventually, to pollen abortion. Zhu et al. (2008) created a mutant of *Arabidopsis thaliana attdf1* using EMS mutagenesis technology. Compared to the tapetum cells of wild *Arabidopsis thaliana*, the tapetum cells of the stamen anthers were swollen, vacuolated, and excessively divided, preventing them from being unable to transform into the secretory tapetum. Simultaneously, callose around the tetrad was deposited for a long time and the microspores could not be released in time, leading to the failure to form pollen grains, resulting in pollen abortion [27]. The tapetum cell development of *ogu*-CMS in black cabbage was studied, and the tapetum cell development characteristics were like those of the rice mutant *ostdf1*. Tapetum vacuoles rapidly form after microspore meiosis, and they cannot secrete enough callose enzyme, so most microspores cannot be released in time. Even if a few microspores are released, the tapetum cells squeeze them until they degenerate and disappear, indicating male sterility. Furthermore, overexpression of the rapeseed *BcTDF1* gene in the *Arabidopsis thaliana attdf1* mutant restored the pollen fertility of the *Arabidopsis thaliana attdf1* mutant to some extent and produced some mature and fertile pollen grains [28]. The ability of the *tdf1*

mutant to induce plant pollen abortion was confirmed in this study. In this study, *TaTDF1* was overexpressed in *Arabidopsis thaliana* and dominant chimerism was used to suppress the silencing of the *TDF1* gene. It was found that the *TaTDF1*-OE and *TDF1*-EAR transgenic lines bloomed normally, and the average bolting time of the *TaTDF1*-OE overexpression lines was 7 d earlier. The results of Alexander staining of the anthers are shown in red. However, the silencing lines of the *TDF1*-EAR dominant chimera suppression delayed the bolting period by an average of 4 d. Its anthers are shriveled and thin, and Alexander staining of the anthers is blue-green. VIGS technology for *TaTDF1* silencing in wheat showed that the anthers of the wheat-silent strain *tatdf1* were shriveled, thin, and dull in the loose pollen stage; the seed-setting rate decreased significantly. DAPI staining of pollen grains revealed abnormal nuclear development, 82.05% were seedless or unable to form normal fish-like sperm nuclei. However, 17.95% of the pollen grains developed into mature and fertile fish-like sperm nuclei (Fig. 19). After 1% I₂-KI staining, most pollen grains were yellow-brown, and a few pollen grains remained blue-black. The results showed that downregulation of *TaTDF1* could induce pollen abortion in wheat. Tapetum cells from the *ostdf1* gene knockout mutant showed a vacuolated phenotype similar to the *Arabidopsis thaliana attdf1* mutant, and TUNEL stained nuclei were not observed in anthers.

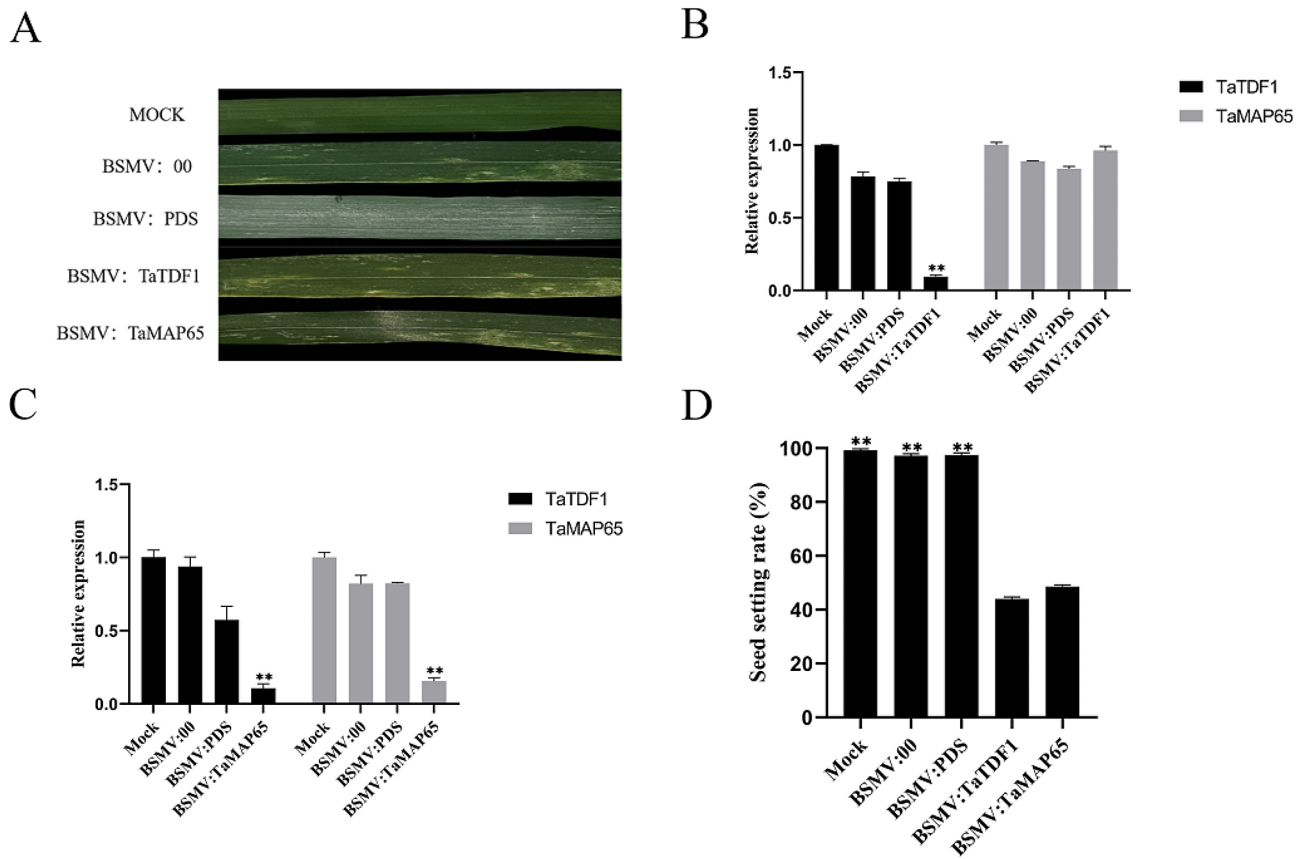


Fig. 15 Silence the functional traits of *TaTDF1* and *TaMAP65* in wheat. **(A)** Wheat leaves were treated with virus constructs for 10 days. Mock, control inoculations; BSMV:00, negative control; BSMV: PDS, positive control. **(B-C)** Gene-silencing efficiency detection after virus-induced silencing. **(B)** The relative transcription levels of anthers *TaMAP65* and *TaTDF1* genes in *tatdf1* silencing strains after BSMV virus infection with flag leaves. **(C)** The relative transcription levels of anthers *TaMAP65* and *TaTDF1* genes in *tamap65* silencing strains after BSMV virus infection with flag leaves. **(D)** The seed setting rate of silent strains after inoculation of flag leaves of BSMV virus. Data was presented as the means \pm SD of three technical replicates and three biological replicates. The significance of differences was assessed using the Student's t-test. ** $p < 0.05$

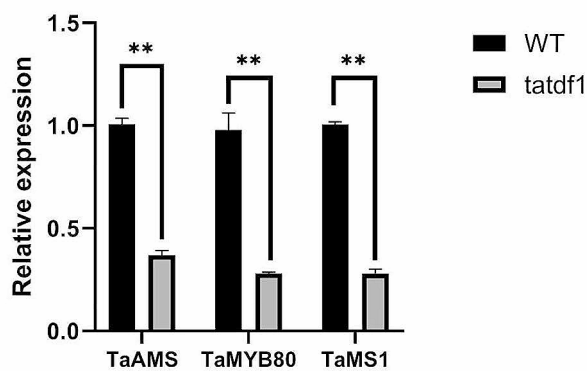


Fig. 16 qRT-PCR analysis of key genes in tapetum development downstream of *TaTDF1* gene. Data was presented as the means \pm SD of three technical replicates and three biological replicates. The significance of differences was assessed using the Student's t-test. ** $p < 0.05$

PCD defects were confirmed in the tapetum cells of *ostdf1* anthers, leading to pollen abortion [18].

In summary, these findings suggest that MYB family transcription factor *TDF1* may play a key role in regulating tapetum development and late function during wheat anther development. Similar to *AtTDF1* of *Arabidopsis thaliana*, *TDF1* affects pollen fertility by regulating tapetal production and degradation. Thus, the process of tapetum development in wheat may be similar to that of *Arabidopsis thaliana*, which is controlled by the conserved genetic pathway *DYT1-TDF1-AMS-MYB80-MS1*. In this study, the protein TaMAP65 interacting with TaTDF1 was screened by yeast two-hybrid test. Further qRT-PCR was performed on *tatdf1* and *tamap65* silent strains, and the results preliminarily indicated that *TaTDF1* was located in the upstream of *TaMAP65*, which was a supplement to the above genetic pathway (Fig. 20). Unfortunately, this study could not further study the regulatory relationship between *DYT1* and *MAP65* to further improve this genetic pathway. The process of pollen abortion in *tatdf1* silenced strains could not be studied



Fig. 17 The phenotypic analysis of the spike and anther after BSMV virus infection. **(A-C)** The phenotype of the spike, reproductive organ and anther after BSMV virus infection. **(A1-A5)** wheatear. **(B1-B5)** pistil and stamen. **(C1-C5)** Anther. **(1)** The phenotype of MOCK wheat. **(2)** The phenotype of BSMV:00-infected wheat. **(3)** The phenotype of BSMV: *PDS*-infected wheat. **(4)** The phenotype of BSMV: *TaTDF1 TaTDF1*-infected wheat. **(5)** The phenotype of BSMV: *TaMAP65 TaMAP65*-infected wheat

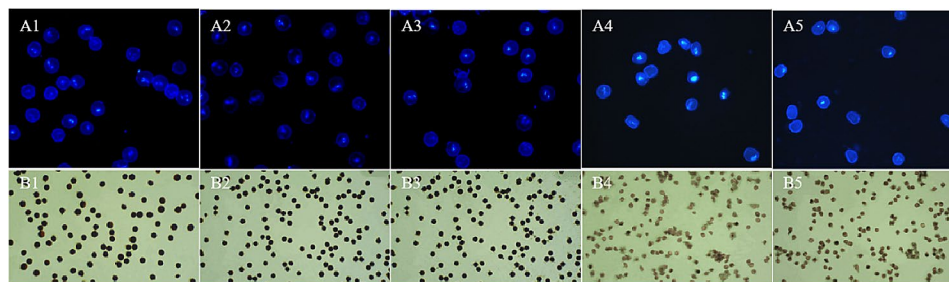


Fig. 18 The phenotypic analysis of the microspore after BSMV virus infection. **(A1-A5)** DAPI staining of microspores in BSMV-infected wheat. **(B1-B5)** I_2 -KI staining of microspores in BSMV-infected wheat. **(1)** The phenotype of MOCK wheat. **(2)** The phenotype of BSMV:00-infected wheat. **(3)** The phenotype of BSMV: *PDS*-infected wheat. **(4)** The phenotype of BSMV: *TaTDF1*-infected wheat. **(5)** The phenotype of BSMV: *TaMAP65*-infected wheat

during the process of tapetum cell development. And their relations could not be illustrated. Compared with MF-90-110, the expression level of *TaTDF1* in MS-90-110 was lower, suggesting that *TaTDF1* may be related to pollen abortion in wheat K-type male sterile lines. This results was confirmed in previous study. Wu et al. (2023) showed that *TaTDRL* (*AtAMS* homolog gene) is down-regulated during the development of anther in MS-90-110 [21]. Meanwhile, *AtTDF1* is the upstream gene of *AtAMS* in *Arabidopsis thaliana*, indicating *TaTDRL* is possibly located at downstream of *TaTDF1*. It can be inferred that *TaTDF1* and *TaTDRL* are also key genes involved in pollen abortion during the development of anther in MS-90-110. But this hypothesis needs further study.

Jasmonic acid (JA) is an important hormone that is widely involved in plant growth and development, metabolic regulation, stress, and defense responses

[29]. Among these, MYB transcription factors promote anther dehiscence by interacting with methyl jasmonate (MeJA) to ensure normal anther development and pollen fertility. Qi et al. (2015) found that the development of JA-mediated stamen and grain setting were regulated by the bHLH-MYB complex. Among them, the bHLH transcription factor *MYC5*, the target gene of the JAZ repressor, plays an important regulatory role in stamen development and grain setting, together with the other bHLH factors *MYC2*, *MYC3*, and *MYC4*. Furthermore, the bHLH transcription factor *MYC5* interacts with the MYB transcription factors *MYB21* and *MYB24* to form a bHLH-MYB transcription complex that synergistically regulates stamen development [30]. The R2R3-MYB transcription factors *MYB21*, *MYB24*, and *MYB108* have been shown to affect stamen development by regulating the JA content. Its abnormal expression can lead to filament elongation, delayed anther dehiscence, and

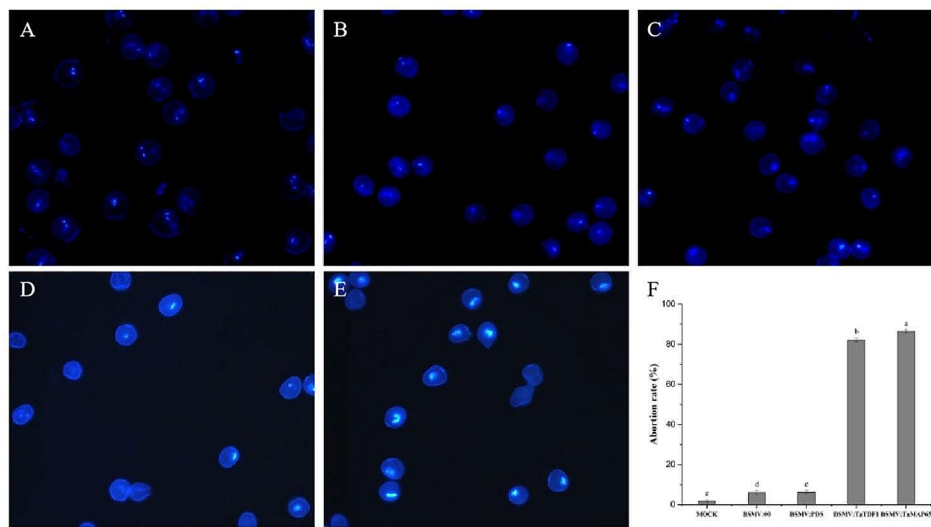


Fig. 19 (A) DAPI staining of microspore in BSMV-infected wheat. The phenotype of MOCK wheat. (B) The phenotype of BMSV:00-infected wheat. (C) The phenotype of BMSV: PDS-infected wheat. (D) The phenotype of BMSV: TaTDF1-infected wheat. (E) The phenotype of BMSV: TaMAP65-infected wheat. (F) The abortion rate of silent strains after inoculation of inverted bilobite of BSMV virus. Data were expressed as the mean ± SD of 3 independent biological replicates. The significance of the differences was assessed using the student t test. $p < 0.05$

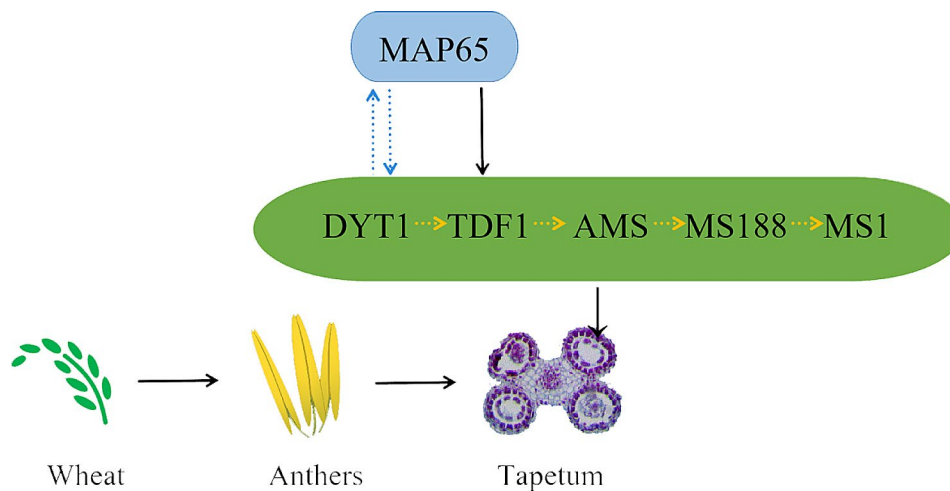


Fig. 20 Genetic pathways during the development of wheat tapetum layer. The solid black arrows represent definite regulatory relationships, the dashed yellow arrows represent conservative regulatory relationships, and the dashed blue arrows represent unclear regulatory relationships

decreased pollen viability, eventually leading to the abortion of male pollen [11, 31, 32]. MYB21 and MYB24 are direct targets of JAZs, and their functions are affected by their content. Once the JA signal was detected, COI1 recruited JAZs into the SCF(COI1) complex and used the 26 S proteasome for ubiquitination and degradation. MYB21 and MYB24 are released to activate the expression of various genes for JA-regulated anther development and filament elongation [11]. Both LoMYB21 in silent lilies and overexpression of LoMYB21 in Arabidopsis caused abnormal JA content and signal transduction, delayed anther dehiscence, reduced Jasmonic acid accumulation, and pollen abortion [33]. On top of that, Abscisic acid (ABA) is also an important plant hormone

that regulates plant resistance to various biotic and abiotic stresses. These include drought, cold, and salt stress, seed dormancy, and pollen fertility [34]. The pollen activity of plants (L4) overexpressing AtNCED3 decreased. The results of semi-thin sections and electron microscope observations of anthers showed that tapetum cells in L4 degraded too fast, microspores could not absorb nutrients, and their pollen fertility decreased. However, after exogenous spraying of ABA, the surface of the wax content on the anther surface increased and nutrients in the tapetum cells were continuously supplied, thus improving the fertility of the pollen grains [35]. The atu2af65b mutant showed an early flowering phenotype under both long- and short-d conditions, and the transcript of the

flowering inhibition gene FLC decreased in the shoot tip of *atu2af65b*. This was mainly because of abnormal splicing of ABI5 and a decrease in transcript abundance. Furthermore, ABA promotes the expression of *AtU2AF65b* during ABA-induced flowering. However, the transition and splicing of FLC and ABI5 in the *atu2af65b* mutant were impaired; therefore, they could not normally induce male germ cell development [36]. Plants overexpressing the ABA-dependent SnRK2 kinase members *SAPK8* and *ABF1* showed delayed flowering. It is more sensitive to exogenous spraying of ABA-mediated flowering inhibition, whereas simultaneously knocking out *ABF1* and its homologous gene *bZIP40* can promote flowering [37]. These results indicate that JA and ABA hormones interact with MYB and bZIP transcription factors, respectively, by recognizing the CGTCA, TGACG-motif, and ABRE (ACGTG/CACGTG) motifs. This interferes with gene expression, affecting pollen fertility. This result is discussed preliminarily in this study.

In this study, the regulatory elements of the *TaTDF1* promoter region were analyzed using PlantCARE and NewPLACE. Two cis-acting regulators, the CGTCA motif and the TGACG-motif, related to the MeJA reaction; one cis-acting regulator, ABRE (ACGTG/CACGTG), related to the ABA reaction; four photoperiod response elements, GT1-motif, ATCT motif, G-box, and GA-motif; and three cis-acting regulators, ARE, GC-motif, and MBS, related to adversity stress, were identified (Fig. 21; Table S4). Among these, MeJA and ABRE cis-acting elements may interact with the upstream MYB and bZIP transcription factors to regulate the development of anthers or pollen grains. Therefore, Yeast One-Hybrid (Y1H) and Electrophoretic Mobility Shift Assay (EMSA) experiments can be used to further study the degradation of transcription factors interacting with MeJA and ABRE elements in *TaTDF1* promoter region in wheat tapetum cells and the regulatory mechanism during anther or pollen grain development. This study

provides new insights into the extraction of key genes that regulate the development of male reproductive organs in wheat.

Materials and methods

Materials

In this study, the wheat K-type cytoplasmic male-sterile line MS (Kots) -90-110 (MS) and its fertile control line MR (Kots) -90-110 (MF) were used. When microspore development reached the meiosis, early uninucleate (Euns), late uninucleate (Luns), binucleate (Bns), and trinucleate (Tns) stages, samples were taken from the field, placed on ice, and brought back to the laboratory for microscopic examination of pollen kernel development. After confirmation, another 30 ears of anther were mixed and placed into 2.0 mL EP tube, and frozen in liquid nitrogen and stored in the refrigerator at -80°C for future use. The wheat variety material used in BSMV-VIGS test was field. The above wheat variety materials Provided by the Key Laboratory of Crop Heterosis Research and Utilization at the Northwest A&F University.

RNA extraction and qRT-PCR analysis

Total RNA was extracted using the Total RNA Extraction Reagent RNA Isolator (Vazyme, Nanjing, China) and was purified according to the manufacturer's instructions. The first strand of cDNA was synthesized using the HiScript[®] II Reverse Transcriptase kit (Vazyme, Nanjing, China), according to the manufacturer's instructions. Real-time quantitative PCR (qRT-PCR) was performed using ChamQ SYBR qPCR Master Mix (Vazyme, Nanjing, China) on Biosystems 7500 Fast Real-Time PCR System. Using an internal reference gene (GenBank accession No. AB181991.1), the relative expression of *TaActin* was calculated according to $2^{-\Delta\Delta C_t}$ method with three biological repeats. Data were analyzed using Duncan's method in SPASS 12.0.

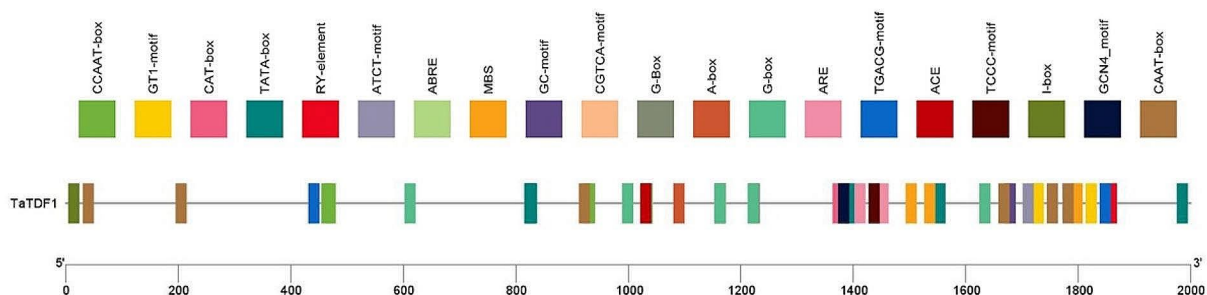


Fig. 21 Promoter cis-regulatory element analysis of *TaTDF1*. The putative plurality of cis-acting elements in the *TaTDF1* promoter region is predicted by PlantCARE

Cloning and sequence analysis of TaTDF1

The OsTDF1 protein sequence was obtained from GenBank (accession number: XP.015630216.1). The nucleotide sequence of *TaTDF1* and its encoded amino acid sequence were retrieved from the NCBI for Biotechnology Information and Ensembl Plant databases. The full-length coding sequence CDS (Table S1) of MF-90-110 during meiosis was amplified with *TaTDF1* gene-specific primers. The PCR product was purified using the Easy-Pure® rapid gel extraction kit (Transgen, China, Beijing). This was connected to the pEASY-T1 cloning vector (Transgen, China, Beijing) to construct a recombinant plasmid, which was then inserted into competent cells of *E. coli* DH5α (Protein Interaction, Wuhan, China). Positive clones were verified by PCR and sequencing (Sheng-gong, China, Shanghai).

Bioinformatic analysis of TaTDF1

TaTDF1 protein sequence. The TaTDF1 protein domain was analyzed using the online tool SMART (<https://smart.embl.de/>). The online software programs PSIPRED (<http://bioinf.cs.ucl.ac.uk/psipred/>) and SWISS-MOLD (<https://swissmodel.expasy.org/interactive>) were used to predict the secondary and tertiary structures of TaTDF1. The physical and chemical properties of TaTDF1 were analyzed using EXPASY (<https://web.expasy.org/prot-param/>) software. The TMHMM Server V.2.0 (<http://www.cbs.dtu.dk/services/TMHMM>) and SignalP-5.0 (<http://www.cbs.dtu.dk/services/SignalP/0>) predicted the transmembrane domain and the signal peptide of the TaTDF1 protein, respectively. MEGA software was used to study the evolutionary relationship of TDF1 in different species. The conserved domain of TaTDF1 was identified by multisequence alignment using DNAMAN software.

Subcellular localization of TaTDF1

The open reading frame of *TaTDF1* was amplified using specific primers (without a stop codon). The PCR product was ligated into the *Bst*BI site of the pCAMBIA1302-GFP (CaMV 35 S promoter) vector. The primers used are listed in Table S1. The fusion and empty control vectors were transferred to *Agrobacterium tumefaciens* strain (GV3101), and the bacteria were introduced to *Nicotiana Benthamiana* leaves for transient expression. GFP signals were observed using a laser confocal fluorescence microscope (Olympus, Tokyo, Japan).

Yeast two-hybrid screening (Y2H) assay

The full-length *TaTDF1* cDNA was cloned using specific primers and attached to the pGBKT7 vector as bait (Table S1). The BD-TaTDF1 recombinant plasmid was transfected into Y2H gold-receptive yeast cells (Protein Interaction, Wuhan, China) using the lithium acetate

conversion method [38]. After the non-toxic and self-activating effects were confirmed using SD/-Trp and SD/-Trp/-Ade/-His media, the successfully transformed positive monoclonal solution was mixed with the wheat anther cDNA library solution and coated onto SD/-Leu/-Trp/-His/-Ade media. It was then combined with X-α-gal chromogenic solution to screen for blue and white spots. Blue-positive clones were amplified by PCR and verified by sequencing (Sheng-gong, China, Shanghai).

Rotation verification assay of TaTDF1 and TaMAP65

Specific primers were designed to clone the full-length cDNA of *TaMAP65* and inserted into the pGADT7 vector (Table S1). BD-TaTDF1, AD-TaMAP65, and recombinant plasmids were co-transformed into Y2HGold yeast receptive cells (Protein Interaction, Wuhan, China) using the lithium acetate conversion method. A positive control (co-transformed AD-T and BD-53 plasmids) and a negative control (co-transformed AD-T and BD-lam plasmids) were used. The interaction between SD/-Trp/-Ade/-Leu/-His medium and X-α-gal color reaction was verified.

Bimolecular-fluorescence complementation (BiFC) assay

The full-length cDNA of *TaTDF1* was cloned into the pUN-SPYNE vector. The full-length cDNA of *TaMAP65* was cloned into the pUC-SPYCE vector (see Table S1 for primer information). PUN-SPYNE, pUC-SPYCE, pUN-TaTDF1, and pUC-TaMAP65 were transformed into *Agrobacterium tumefaciens* strain GV3101 (pSoup-19), which was then introduced into *Nicotiana Benthamiana* leaves for transient expression. GFP signals were observed using confocal laser fluorescence microscopy (Olympus, Tokyo, Japan).

Genetic transformation of *Arabidopsis thaliana*

The CDS of *TaTDF1* was cloned and inserted between the *Nco*I and *Spe*I cleavage sites of the pCAMBIA1302 vector to construct the *TaTDF1* overexpression vector, and p35S::TaTDF1 (*TaTDF1*-OE) was obtained. The EAR motif contains two distinct conservation patterns: L/FDLNL/F(x)P and LxLxL. Through negatively regulating expression of genes involved in development, abiotic and biotic stress responses, plants can keep suitable physiological states under different environmental conditions [39]. To construct a chimeric suppressor of *TaTDF1*, we fused *TaTDF1* CDSs with coding EAR motif (LDLDLELRLGFA) suppressor domain (RD) DNA. Subsequently, it was inserted into the downstream 35 S promoter of the pCAMBIA1302 vector to construct the p35S::TaTDF1 (*TaTDF1*-EAR) fusion vector. The primers used are listed in Supplementary Table S1 A. *Agrobacterium tumefaciens* with recombinant plasmids *TaTDF1*-OE and *TaTDF1*-EAR were used to infect *Arabidopsis thaliana* floss using

the flower impregnation method to obtain *Arabidopsis thaliana* positive plants.

Gene silencing of TaTDF1, TaMAP65 in wheat

The BSMV comprises three righteous RNA strands, α , β , and γ . Specific primers were designed to clone conserved cDNA fragments of *TaTDF1* (+95–+188) and *TaMAP65* (+483–+589), and were inserted into γ vector by the restriction endonucleases *PacI* and *NotI* (see Table S1 for primer information). α , β , γ , γ -PDS, γ -*TaTDF1*, and γ -*TaMAP65* recombinant plasmids were digested by a single enzyme (Table S2). In vitro transcription was performed using the T7 High-Yield RNA Synthesis Kit (Sheng Gong, China, Shanghai).

α , β , γ , γ -PDS, γ -*TaTDF1*, and γ -*TaMAP65* transcribed in vitro were mixed on ice according to the volume of α : β : γ (γ -PDS/ γ -*TaTDF1*/ γ -*TaMAP65*):GPK buffer=0.5:0.5:0.5:9 (10.5 μ L). The flag leaf and inverted wheat leaf were infected with recombinant virus, and then cultured in greenhouse under the conditions of 25 °C, 16 h light, 20 °C and 8 h darkness. After 7–10 d of inoculation, symptoms were observed, and photos were taken. When the pollen of infected plants developed into the binucleate and trinucleate stages, the silencing efficiency of *TaTDF1* and *TaMAP65* in Mock and silenced plants was detected by qRT-PCR.

Supplementary Information

The online version contains supplementary material available at <https://doi.org/10.1186/s12870-024-05456-z>.

Supplementary Material 1: Fig S1. Hydrophathy and Secondary structure analysis of TaTDF1 protein. Fig S2. Hydrophathy and Secondary structure analysis of TaMAP65 protein. Fig S3. Predicted 3D structure of TaTDF1, TaMAP65 proteins.

Supplementary Material 2: Table S1. Primers used in this study.

Supplementary Material 3: Table S2. Linearization of VIGS plasmids.

Supplementary Material 4: Table S3. Prediction of physicochemical properties of TaTDF1 and TaMAP65 protein; The results of TaTDF1 protein yeast two-hybrid sieve library.

Supplementary Material 5: Table S4. Cis-elements in the upstream regulation region of *TaTDF1* gene.

Acknowledgements

Wheat materials used in this study were provided by Shaanxi Key Laboratory of Crop Heterosis. We would like to appreciate the Innovation Center for Crop Biology staff for technical assistance.

Author contributions

S.S., and P.T. contributed equally to this work. Y.S. managed the project. Y.S. and N.N. conceived and designed the experiments. S.S., and P.T. carried out the experiments and analyzed datum. S.S., and Y.S. wrote and finalized the manuscript, with the advice from G.Z. R.W., Y.R., and N.Y. involved in anther collection, RNA extraction, and phenotype investigation. B.W. carried out field experiment and gave some important suggestions for improving the design of the experiments. All authors have read and approved the manuscript.

Funding

The design of the study, sample collection, genes identification and analysis, gene quantification, interpretation of data and the writing of the manuscript was financially supported by National Natural Science Foundation of China (No.31701500); Shaanxi Province Key Research and Development Program General Project (No.2022NY-176); Fundamental Research Funds of Northwest A&F University (No.1090322148); Ph.D. Start-up Fund of Northwest A&F University (No.2452015263); the Fundamental Research Funds for the Central Universities (2452022109); Yangling Seed Industry Innovation Key Research and Development(Ylzy-xm-03); The Programme of Introducing Talents of Innovative Discipline to Universities (Project 111) from the State Administration of Foreign Experts Affairs (#B18042) "Crop breeding for disease resistance and genetic improvement".

Data availability

The datasets generated and/or analysed during the current study are available in the NCBI for Biotechnology Information and Ensembl Plant databases, <https://www.ncbi.nlm.nih.gov/protein/2123818813> or https://plants.ensembl.org/Triticum_aestivum/Gene/Summary?db=core;g=TraesCS4D02G192400;r=4D:335348356-335350211;t=TraesCS4D02G192400.1;tl=vmsH3X08cDFPfav-23316136-2607265691.

Declarations

Ethics approval and consent to participate

Experimental research and field studies on plants (either cultivated or wild), including the collection of plant material, must comply with relevant institutional, national, and international guidelines and legislation.

Consent for publication

Not applicable.

Competing interests

The authors declare no competing interests.

Received: 4 November 2023 / Accepted: 26 July 2024

Published online: 05 August 2024

References

- Senapati N, Semenov MA, Halford NG, Hawkesford MJ, Asseng S, Cooper M, Ewert F, van Ittersum MK, Martre P, Olesen JE, Reynolds M, Rötter RP, Webber H. Global wheat production could benefit from closing the genetic yield gap. *Nat Food*. 2022;3:532–41. <https://doi.org/10.1038/s43016-022-00540-9>.
- Zhang MH, Yu JZ, Xie QJ, Wen SZ, Li JH, Bi C, Xie CJ, Ni ZF, Liang RQ, You MS. The male sterility of bread wheat line XN291S was resulted from the deletion of a large segment at the end of 6BS. *Euphytica*. 2023;219:62. <https://doi.org/10.1007/s10681-023-03191-4>.
- Huang SN, Peng SL, Liu ZY, Li CY, Tan C, Yao RP, Li DY, Li X, Hou L, Feng H. Investigation of the genes associated with a male sterility mutant (msm) in Chinese cabbage (*Brassica campestris* ssp. *pekinensis*) using RNA-Seq. *Mol Genet Genomics*. 2020;295:233–49. <https://doi.org/10.1007/s00438-019-01618-z>.
- Xu C, Xu Y, Wang Z, Zhang X, Wu Y, Lu X, Sun H, Wang L, Zhang Q, Zhang Q, Li X, Xiao J, Li X, Zhao M, Ouyang Y, Huang X, Zhang Q. (2023) Spontaneous movement of a retrotransposon generated genic dominant male sterility providing a useful tool for rice breeding. *Natl Sci Rev*. 7;10(9):nwad210. <https://doi.org/10.1093/nsr/nwad210>
- Zheng XL, He LL, Liu Y, Mao YW, Wang CQ, Zhao BL, Li YH, He H, Guo SQ, Zhang LS, Schneider H, Tadege M, Chang F, Chen JH. A study of male fertility control in *Medicago truncatula* uncovers an evolutionarily conserved recruitment of two tapetal bHLH subfamilies in plant sexual reproduction. *New Phytol*. 2020;228:1115–33. <https://doi.org/10.1111/nph.16770>.
- Yuan Y, Yang XP, Feng MF, Ding HY, Khan MT, Zhang JS, Zhang MQ. Genome-wide analysis of R2R3-MYB transcription factors family in the autopolyploid *Saccharum spontaneum*: an exploration of dominance expression and stress response. *BMC Genomics*. 2021;22:622. <https://doi.org/10.1186/s12864-021-07689-w>.

7. Li JL, Han GL, Sun CF, Sui N. Research advances of MYB transcription factors in plant stress resistance and breeding. *Plant Signal Behav.* 2019;14:1613131. <https://doi.org/10.1080/15592324.2019.1613131>.
8. Jiang CK, Rao GY. Insights into the diversification and evolution of R2R3-MYB transcription factors in plants. *Plant Physiol.* 2020;183:637–55. <https://doi.org/10.1104/pp.19.01082>.
9. Wu Y, Wen J, Xia YP, Zhang LS, Du H. Evolution and functional diversification of R2R3-MYB transcription factors in plants. *Hortic Res.* 2022;9:uhac058. <https://doi.org/10.1093/hr/uhac058>.
10. Millar AA, Gublera F. The Arabidopsis GAMYB-Like genes, MYB33 and MYB65, are MicroRNA-Regulated genes that redundantly facilitate Anther Development. *Plant Cell.* 2005;17:705–21. <https://doi.org/10.1105/tpc.104.027920>.
11. Song SS, Qi TC, Huang H, Ren QC, Wu DW, Chang CQ, Peng W, Liu YL, Peng JR, Xie DX. The Jasmonate-ZIM Domain proteins interact with the R2R3-MYB transcription factors MYB21 and MYB24 to Affect Jasmonate-Regulated Stamen Development in Arabidopsis. *Plant Cell.* 2011;23:1000–13. <https://doi.org/10.1105/tpc.111.083089>.
12. Cheng H, Song SS, Xiao LT, Soo HM, Cheng ZW, Xie DX, Peng JR. Gibberellin acts through jasmonate to control the expression of MYB21, MYB24, and MYB57 to promote stamen filament growth in Arabidopsis. *PLoS Genet.* 2009;5:e1000440. <https://doi.org/10.1371/journal.pgen.1000440>.
13. Ferguson AC, Pearce S, Band LR, Yang CY, Ferjentsikova I, King J, Yuan Z, Zhang DB, Wilson ZA. Biphasic regulation of the transcription factor ABORTED MICROSPORES (AMS) is essential for tapetum and pollen development in Arabidopsis. *New Phytol.* 2017;213:778–90. <https://doi.org/10.1111/nph.14200>.
14. Lei T, Zhang LS, Feng P, Liu Y, Yin WZ, Shang LN, He GH, Wang N. OsMYB103 is essential for tapetum degradation in rice. *Theor Appl Genet.* 2022;135:929–45. <https://doi.org/10.1007/s00122-021-04007-6>.
15. Liu XZ, Jiang YL, Wu SW, Wang J, Fang CW, Zhang SW, Xie RR, Zhao LN, An XL. The ZmMYB84-ZmPKSB regulatory module controls male fertility through modulating anther cuticle—pollen exine trade-off in maize anthers. *Plant Biotechnol J.* 2022;20:2342–56. <https://doi.org/10.1111/pbi.13911>.
16. Zhu J, Lou Y, Xu XF, Yang ZN. A genetic pathway for Tapetum development and function in Arabidopsis. *J Integr Plant Biol.* 2011;53:892–900. <https://doi.org/10.1111/j.1744-7909.2011.01078.x>.
17. Gu JN, Zhu J, Yu Y, Teng XD, Lou Y, Xu XF, Liu JL, Yang ZN. DYT1 directly regulates the expression of TDF1 for tapetum development and pollen wall formation in Arabidopsis. *Plant J.* 2014;80:1005–13. <https://doi.org/10.1111/tbj.12694>.
18. Cai CF, Zhu J, Lou Y, Guo ZL, Xiong SX, Wang K, Yang ZN. The functional analysis of OsTDF1 reveals a conserved genetic pathway for tapetal development between rice and Arabidopsis. *Sci Bull.* 2015;60:1073–82. <https://doi.org/10.1007/s11434-015-0810-3>.
19. Wu SY, Hou LL, Zhu J, Wang YC, Zheng YL, Hou JQ, Yang ZN, Lou Y. Ascorbic acid-mediated reactive oxygen species homeostasis modulates the switch from tapetal cell division to cell differentiation in Arabidopsis. *Plant Cell.* 2023;35:1474–95. <https://doi.org/10.1093/plcell/koad037>.
20. Moriyama T, Shea DJ, Yokoi N, Imakiire S, Saito T, Ohshima H, Saito H, Okamoto S, Fukai E, Okazaki K. Identification of a male sterile candidate gene in *Lilium x formolongi* and transfer of the gene to Easter Lily (*L. longiflorum*) via hybridization. *Front Plant Sci.* 2022;13:914671. <https://doi.org/10.3389/fpls.2022.914671>.
21. Wu BL, Xia Y, Zhang GS, Wang JW, Ma SC, Song YL, Yang ZQ, Dennis ES, Niu N. The transcription factors TaTDR1 and TaMYB103 synergistically activate the expression of TAA1a in wheat, which positively regulates the development of Microspore in Arabidopsis. *Int J Mol Sci.* 2022;23:7996. <https://doi.org/10.3390/ijms23147996>.
22. Wang JL, Wang HB, Yang HQ, Hu RL, Wei DY, Tang QL, Wang ZM. The role of NAC transcription factors in flower development in plants. *Chin J Biotechnol.* 2022;38:2687–99. <https://doi.org/10.13345/j.cjb.210943>.
23. Parish RW, Li SF. Death of a tapetum: a programme of developmental altruism. *Plant Sci.* 2010;178:73–89. <https://doi.org/10.1016/j.plantsci.2009.11.001>.
24. Wang YK, Ye H, Bai JF, Ren F. The regulatory framework of developmentally programmed cell death in floral organs: a review. *Plant Physiol Biochem.* 2021;158:103–12. <https://doi.org/10.1016/j.plaphy.2020.11.052>.
25. Jeong HJ, Kang JH, Zhao MA, Kwon JK, Choi HS, Bae JH, Lee HA, Joung YH, Choi D, Kang BC. Tomato Male sterile 1035 is essential for pollen development and meiosis in anthers. *J Exp Bot.* 2014;65:6693–709. <https://doi.org/10.1093/jxb/eru389>.
26. Liu XY, Yang MX, Liu XL, Wei K, Cao X, Wang XT, Wang XX, Guo YM, Du YC, Li JM, Liu L, Shu JS, Qin Y, Huang ZJ. A putative bHLH transcription factor is a candidate gene for male sterile 32, a locus affecting pollen and tapetum development in tomato. *Hortic Res.* 2019;6:88. <https://doi.org/10.1038/s41438-019-0170-2>.
27. Zhu J, Chen H, Li H, Gao JF, Jiang H, Wang C, Guan YF, Yang ZN. Defective in Tapetal Development and function 1 is essential for anther development and tapetal function for microspore maturation in Arabidopsis. *Plant J.* 2008;55:266–77. <https://doi.org/10.1111/j.1365-3113X.2008.03500.x>.
28. Zhang SY, Wang J, Chen GH, Ye XY, Zhang L, Zhu SD, Yuan LY, Hou JF, Wang CG. Functional analysis of a MYB transcription factor BrTDF1 in the tapetum development of Wucai (*Brassica rapa* Ssp). *Sci Hort.* 2019;257:108728. <https://doi.org/10.1016/j.scienta.2019.108728>.
29. Wang J, Song L, Gong X, Xu JF, Li MH. Functions of Jasmonic Acid in Plant Regulation and response to Abiotic Stress. *Int J Mol Sci.* 2020;21(4):1446. <https://doi.org/10.3390/ijms21041446>.
30. Qi TC, Huang H, Song SS, Xie DX. Regulation of jasmonate-mediated Stamen development and seed production by a bHLH-MYB complex in Arabidopsis. *Plant Cell.* 2015;27:1620–33. <https://doi.org/10.1105/tpc.15.00116>.
31. Mandaokar A, Thines B, Shin B, Lange BM, Choi G, Koo YJ, Yoo YJ, Choi YD, Choi G, Browse J. Transcriptional regulators of stamen development in Arabidopsis identified by transcriptional profiling. *Plant J.* 2006;46:984–1008. <https://doi.org/10.1111/j.1365-3113X.2006.02756.x>.
32. Mandaokar A, Browse J. MYB108 acts together with MYB24 to regulate jasmonate-mediated stamen maturation in Arabidopsis. *Plant Physiol.* 2009;149:851–62. <https://doi.org/10.1104/pp.108.132597>.
33. Tong Z, Dong TT, Li QH, Wang R, He JN, Hong B. R2R3-type LoMYB21 affects jasmonate-regulated development and dehiscence of anthers in lily (*Lilium orientalis* hybrids). *Hortic Plant J. S* 2023;2468–0141 (23):00065–1. <https://doi.org/10.1016/j.hpj.2023.04.004>.
34. Chen K, Li GJ, Bressan RA, Song CP, Zhu JK, Zhao Y. Abscisic acid dynamics, signaling, and functions in plants. *J Integr Plant Biol.* 2020;62:25–54. <https://doi.org/10.1111/jipb.12899>.
35. Liu JL, Chen H. Effects of exogenous ABA on anther development and cutin wax in rice. *Shanxi Normal Univ.* 2019;5:1–46. <https://kns.cnki.net/KCMS/detail/detail.aspx?dbname=CMFD201901&filename=1017279805.nh>.
36. Xiong F, Ren JJ, Yu Q, Wang YY, Lu CC, Kong LJ, Otegui MS, Wang XL. AtU2AF65b functions in abscisic acid mediated flowering via regulating the precursor messenger RNA splicing of ABI5 and FLC in Arabidopsis. *New Phytol.* 2019;223:277–92. <https://doi.org/10.1111/nph.15756>.
37. Tang LQ, Li GH, Wang HM, Zhao J, Li ZY, Liu XX, Shu YZ, Liu WN, Wang S, Huang J, Ying JZ, Tong XH, Yuan WY, Wei XJ, Tang SQ, Wang YF, Bu QY, Zhang J. Exogenous abscisic acid represses rice flowering via SAPP8-ABF1-Ehd1/Ehd2 pathway. *J Adv Res.* 2023;2300175–3. <https://doi.org/10.1016/j.jare.2023.06.012>. 1: S2090-1232.
38. Gietz RD, Schiestl RH. High-efficiency yeast transformation using the LiAc/SS carrier DNA/PEG method. *Nat Protoc.* 2007;2:31–4. <https://doi.org/10.1038/nprot.2007.13>.
39. Kagale S, Rozwadowski K. EAR motif-mediated transcriptional repression in plants: an underlying mechanism for epigenetic regulation of gene expression. *Epigenetics.* 2011;6(2):141–6. <https://doi.org/10.4161/epi.6.2.13627>.

Publisher's Note

Springer Nature remains neutral with regard to jurisdictional claims in published maps and institutional affiliations.